ELSEVIER

Brachytherapy xxx (xxxx) xxx

BRACHYTHERAPY

The American Brachytherapy Society consensus statement for permanent implant brachytherapy using Yttrium-90 microsphere radioembolization for liver tumors

Navesh K. Sharma[1], S. Cheenu Kappadath[2], Michael Chuong[3], Michael Folkert[4], Peter Gibbs[5], Salma K. Jabbour[6], D. Rohan Jeyarajah[7], Andrew Kennedy[8], David Liu[9], Joshua E. Meyer[10], Justin Mikell[11], Rahul S. Patel[12], Gary Yang[13], Firas Mourtada[14,15,*]

[1] *Department of Radiation Oncology, Penn State Hershey School of Medicine, Hershey, PA*
[2] *Department of Imaging Physics, UT MD Anderson Cancer Center, Houston, TX*
[3] *Department of Radiation Oncology, Miami Cancer Institute, Miami, FL*
[4] *Northwell Health Cancer Institute, Radiation Medicine at the Center for Advanced Medicine, New Hyde Park, NY*
[5] *Personalised Oncology Division, Walter and Eliza Hall Institute, Melbourne, Victoria, Australia*
[6] *Rutgers Cancer Institute of New Jersey, Rutgers University, New Brunswick, NJ*
[7] *TCU and UNTHSC School of Medicine, Fort Worth, TX*
[8] *Sarah Cannon Cancer Institute, Nashville, TN*
[9] *Vancouver General Hospital, Vancouver, British Columbia, Canada*
[10] *Fox Chase Cancer Center, Philadelphia, PA*
[11] *University of Michigan, Ann Arbor, MI*
[12] *Icahn School of Medicine at Mount Sinai, New York, NY*
[13] *Loma Linda University, Loma Linda, CA*
[14] *Helen F. Graham Cancer Center & Research Institute, Christiana Care Health System, Newark, DE*
[15] *Department of Radiation Oncology, Sidney Kimmel Cancer Center at Thomas Jefferson University, Philadelphia, PA*

ABSTRACT

PURPOSE: To develop a multidisciplinary consensus for high quality multidisciplinary implementation of brachytherapy using Yttrium-90 (^{90}Y) microspheres transarterial radioembolization (^{90}Y TARE) for primary and metastatic cancers in the liver.

METHODS AND MATERIALS: Members of the American Brachytherapy Society (ABS) and colleagues with multidisciplinary expertise in liver tumor therapy formulated guidelines for ^{90}Y TARE for unresectable primary liver malignancies and unresectable metastatic cancer to the liver. The consensus is provided on the most recent literature and clinical experience.

RESULTS: The ABS strongly recommends the use of ^{90}Y microsphere brachytherapy for the definitive/palliative treatment of unresectable liver cancer when recommended by the multidisciplinary team. A quality management program must be implemented at the start of ^{90}Y TARE program development and follow-up data should be tracked for efficacy and toxicity. Patient-specific dosimetry optimized for treatment intent is recommended when conducting ^{90}Y TARE. Implementation in patients on systemic therapy should account for factors that may enhance treatment related toxicity without delaying treatment inappropriately. Further management and salvage therapy options including retreatment with ^{90}Y TARE should be carefully considered.

CONCLUSIONS: ABS consensus for implementing a safe ^{90}Y TARE program for liver cancer in the multidisciplinary setting is presented. It builds on previous guidelines to include recommendations for appropriate implementation based on current literature and practices in experienced centers. Practitioners and cooperative groups are encouraged to use this document as a guide to formulate their clinical practices and to adopt the most recent dose reporting policies that are critical for a unified outcome analysis of future effectiveness studies.

Keywords: Yttrium-90; Microspheres; Transarterial radioembolization; Metastatic liver cancer; Brachytherapy

Received 20 December 2021; received in revised form 25 March 2022; accepted 14 April 2022; Available online xxx

* Corresponding author: Department of Radiation Oncology, Sidney Kimmel Cancer Center at Thomas Jefferson University, Philadelphia, PA. Office: 215-955-7938; Fax: 215-503-7206.

E-mail address: Firas.Mourtada@jefferson.edu (F. Mourtada).

1538-4721/$ - see front matter
https://doi.org/10.1016/j.brachy.2022.04.004

Please cite this article as: N.K. Sharma *et al.*, The American Brachytherapy Society consensus statement for permanent implant brachytherapy using Yttrium-90 microsphere radioembolization for liver tumors, Brachytherapy, https://doi.org/10.1016/j.brachy.2022.04.004

Nomenclature and abbreviations

ABS	American Brachytherapy Society
ASTRO	American Society for Radiation Oncology
BCLC	Barcelona clinic liver cancer
BED	Biologically effective dose
BT	Brachytherapy
Bq	Becquerel
BSA	Body surface area
CBCT	Cone beam computed tomography
CT	Computed tomography
CTV	Clinical target volume
DVK	Dose-voxel kernel
DPK	Dose-point kernel
DVH	Dose volume histogram
EBRT	External beam radiotherapy
EQD2	Equivalent dose delivered in 2 Gy fractions
FDG	Fluorodeoxyglucose
FMEA	Failure modes and effects analysis
FOV	Field-of-view
GMS	Glass microspheres
GTV	Gross tumor volume
HAI	Hepatic artery infusion
HDR	High-dose-rate
HCC	Hepatocellular carcinoma
IFU	Instruction for use pamphlet
IDA	Iminodiacetic acid agent
ICRU	International Commission on Radiation Units and Measurements
kV	Kilovoltage
LD	Lung mean dose
LDR	Low-dose-rate
LDM	Local deposition method
LSF	Lung shunt fraction
M_{lung}	Lung mass
MBDCA	Model-based dose calculation algorithm
mCRC	Metastatic colorectal cancer
MR	Magnetic resonance
MIRD	Committee on Medical Internal Radiation Dose
MAA	^{99}mTc macroaggregated albumin
MRI	Magnetic resonance imaging
NCCN	National Comprehensive Cancer Network
NRG	This is a national clinical trials network group.
OAR	Organ at risk
PBT	Proton beam therapy
PET	Positron emission tomography
PM	Partition model
PTV	Planning target volume
PVE	Portal vein embolization
TAS102	Fluorothymidine agent
TACE	Transarterial chemoemobilzation
TARE	Trans Arterial Radio Embolization
TI	Tumor involvement
TNR	Tumor compartment compared to the normal liver
QA	Quality Assurance
QC	Quality Control
QM	Quality Management
QMP	Qualified Medical Physicist
RFA	Radiofrequency ablation
RILD	Radiation induced liver disease
RMS	Resin microspheres
ROI	Region of interest
RS/L	Radiation segmentectomy / lobectomy
RTOG	Radiation Therapy Oncology Group
SABR	Stereotactic ablative radiotherapy
SBRT	Stereotactic body radiotherapy
SMA	Superior mesenteric angiogram
SNR	Signal-to-noise ratio
SPECT/CT	Single photon emission computed tomography/computed tomography
TG	Task group
TPS	Treatment planning system
TOF	Time of flight
TRUS	Trans-rectal ultrasound
US	Ultrasound
VSV	voxel-S-values
^{90}Y	Yttrium-90

Introduction

Transarterial Radioembolization (TARE), also sometimes known as Selective Internal Radiation Therapy (SIRT) is a brachytherapy modality that exploits the unique characteristics of cancer angiogenesis through the delivery of radioactive microspheres into tumoral vasculature via trans-arterial infusion of radioactive microspheres (1). The carrier-based delivery of radiation to the tumor is facilitated through the selective infusion/embolization into the hepatic artery, which is the major blood supply to tumor (as opposed to the surrounding liver parenchyma, which receives blood predominantly from the portal venous system). This differential of vascular capacitance serves as the anatomical basis for the resultant deposition of many-folds higher microsphere concentration (and radiation dose) within the tumor. Through selective lobar or segmental vascular catheterization, optimization of TARE delivery can be achieved, and through modulation of the amount and the specific activity of the deposited microspheres, tumoricidal doses of radiation can be delivered whilst minimizing radiobiological effects to the adjacent parenchyma (2,3). The goal of this report is to develop ABS consensus statement for high quality and judicious clinical multidisciplinary implementation of catheter di-

Please cite this article as: N.K. Sharma *et al.*, The American Brachytherapy Society consensus statement for permanent implant brachytherapy using Yttrium-90 microsphere radioembolization for liver tumors, Brachytherapy, https://doi.org/10.1016/j.brachy.2022.04.004

Table 1
Summary of ^{90}Y-radioembolization device properties.

Device	Name	SIR-spheres	TheraSpheres
	manufacturer	Sirtex medical,Woburn, MA, USA	Boston scientific,Marlborough, MA, USA
Radionuclide characteristics	Radionuclide	Yttrium-90	
	Half-life	64.1 h	
	Beta Emission (E_{max})	2.23 MeV (100%)	
	Gamma emission	–	
Microsphere characteristics	Material	Resin	Glass
	Density	1.6 g/cc	3.3 g/cc
	Size range	20-60 μm	20-30 μm

rected brachytherapy using Yttrium-90 (^{90}Y) microsphere TARE for liver cancer.

Methods and materials

The ABS Board of Directors appointed a group of physicians and medical physicists with expertise in ^{90}Y microspheres for liver cancer TARE brachytherapy to provide a consensus statement. A literature review was performed using PubMed and other online search tools to evaluate human clinical studies available in English language for liver disease treatment. The goal of the guidelines, based on the literature review and clinical expertise, is to provide guidance for ^{90}Y TARE brachytherapy workflow including a description of currently available sources, patient selection, imaging (pre- and post-injection), treatment planning and dosimetry, and radiation safety considerations. The report also expanded on the expanding role of ^{90}Y TARE brachytherapy with other treatment modalities such as external beam, high-dose-rate brachytherapy, protons, surgery, systemic agents, and immunotherapy. The results of the ABS consensus committee based on review of the literature, our clinical experience, and collective judgment are as follows.

^{90Y} *Radionuclide physical characteristics*

Commercially available TARE uses ^{90}Y, which is a high energy pure beta emitter that decays with a half-life of 64.2 h to the stable daughter Zirconium-90. The beta particles have a maximum energy of 2.28 MeV, average energy of 0.935 MeV, maximum range in tissue of 11 mm and average range in tissue of 2.5 mm (4).

^{90Y} *Microsphere devices*

There are two radioactive microsphere medical devices currently approved by the United States Food and Drug Administration (FDA) for liver-directed radioembolization. Besides differences in physical characteristics, the devices have different indications. Glass microspheres (GMS) (*Theraspheres*, Boston Scientific, Marlborough, MA) are FDA approved for treatment of unresectable hepatocellular carcinoma (HCC), unresectable HCC tumors that are 1–8 cm in diameter in patients with mild or asymptomatic cirrhosis. They are also used to treat people with unresectable HCC whose cancer has not progressed. Resin microspheres (RMS) (*SIR-Spheres* (SIRTeX Medical, Woburn, MA) are FDA approved for the treatment of unresectable metastatic colorectal cancers with adjuvant intrahepatic floxuridine. Both GMS and RMS devices are routinely used off-label in the treatment of a variety of hypervascular liver tumors including primary HCC and liver metastases from colorectal cancer, neuroendocrine tumors, uveal melanoma, breast cancers, etc. A summary of ^{90}Y-radioembolization device properties is shown in **Table 1**.

1) *TheraSphere* (Boston Scientific, Marlborough, MA) GMS have a mass density of approximately 3.3 g/cm^3 and are 20 to 30 μm diameter glass microspheres with ^{90}Y as an integral constituent (5,6). The spheres are initially manufactured with ^{89}Y incorporated throughout a glass matrix and then through neutron irradiation undergoes ^{89}Y (n,γ) ^{90}Y for activation to the therapeutic form (7). This provides a high nominal activity of 2500 Bq/sphere on the day of calibration (arbitrarily defined as Sunday 1200 h EST). The sphere nominal activity is 1150 Bq/sphere and 110 Bq/sphere at 3 and 12 days postcalibration, respectively. Vials of activity are available from the manufacturer on the calibration date containing 3−20 GBq in increments of 0.5 GBq; the activities on the calibration date equate to approximately 1.2−8 million microspheres. The small number of spheres has a negligible embolic effect. They are administered by injecting saline through the administration kit at 20 cm^3/min, and infusion times are typically less than 5 min. Activities are determined using package insert single-compartment organ level dosimetry to the perfused volume which is usually a lobe or segment(s).
2) *SIR-Spheres*® (SIRTeX Medical, Woburn, MA) RMS have a mass density around 1.6 g/ cm^3 with 90% of the spheres having diameters between 30 and 35 μm (8). ^{90}Y originating from a ^{90}Sr/^{90}Y generator is precipitated as ^{90}Y phosphate salt attached

Please cite this article as: N.K. Sharma *et al.*, The American Brachytherapy Society consensus statement for permanent implant brachytherapy using Yttrium-90 microsphere radioembolization for liver tumors, Brachytherapy, https://doi.org/10.1016/j.brachy.2022.04.004

onto the surface of a cation resin matrix through ion exchange (9). Vials of resin spheres contain 40–80 million microspheres with specific activity of 37.5−75 Bq/sphere. The vendor supplies a 3 GBq vial of microspheres and the user then draws the desired activity which must be used within 24 h of the calibration date (arbitrarily defined as 1800 h EST, on the anticipated day of administration to the patient) (10). The large number of resin spheres has a micro embolic effect. However, the vendor of resin spheres recently introduced an option to receive and treat with vials up to 3 days before calibration which can be used to deliver the same activity with a smaller number of spheres. Infusion with resin requires a slow and pulsatile injection technique to avoid stasis and reflux, which are monitored during infusions with nonionic contrast. The spheres are administered using sterile water or dextrose 5% + sterile water (D5W). The latter is reported to have reduced vasospasms believed to occur from endothelial injury due to osmotic differences between vasculature and sterile water; the end result being fewer infusions terminated due to stasis and less patient pain reported (11–13). Activity to administer is determined using body surface area (BSA) or partition model (PM). Although most users initially opted for BSA due to its simplicity, there is now a trend toward adoption of the PM.

Patient selection

Optimal patient selection is critical for the successful treatment of primary and metastatic liver disease with radioembolization. This selection is context dependent and will vary based on multiple factors such as the histology of the tumor being treated, the availability or lack of active systemic therapy options, the distribution of the patient's disease, the patient's performance status, and the patient's baseline liver function.

Disease histology is important, as the metastatic pattern of various diseases differ, with an impact on the importance of control of any liver involvement in the metastatic setting. For instance, metastatic colorectal cancer can commonly be found only in the liver (14). As this disease is sensitive to multiple systemic agents, control of liver disease may be crucial for durable control of disease and potential improvement of disease-free survival (15,16). In contrast, whereas metastatic pancreatic cancer is frequently seen in the liver, it rarely remains confined to the liver, and sole use of localized treatment of this organ (17) is undertaken at the risk of undertreating extrahepatic disease (18,19). Although occasionally appropriate, this should be performed only in rare clinical circumstances and after multidisciplinary discussion in this and other disease types where widespread metastatic disease can be managed by other mechanisms. Treatment of primary HCC with radioembolization is appropriate to consider in patients who have disease confined to the liver and may be appropriate in those with liver-dominant disease as well, due to the potential positive impact of controlling hepatic disease in these patients.

The distribution of disease within and outside the liver is important to consider in identifying patients for radioembolization. The recommended approach is to first consider whether patients are good candidates for liver-directed therapy of any form. Nonsurgical options for more limited disease may include interventional radiology-based therapies (e.g. radiofrequency ablation, microwave ablation, cryotherapy), interstitial HDR brachytherapy, external beam radiation therapy (e.g. stereotactic ablative radiotherapy—SABR, conventional or hypo fractionated radiation therapy, proton therapy), other embolic therapies (chemoembolization or bland embolization) or alternative regional therapies such as hepatic artery infusion pump therapy. In multiple studies, patients with liver-only disease seem to derive greater benefit from hepatic directed treatment, such as radioembolization, than those with liver-dominant disease (20–24). One challenge is that the liver-dominant state does not have an agreed-upon definition and is often variably interpreted. The FOXFIRE trial proposed "limited extra-hepatic disease, defined as ≤5 nodules in the lung and/or one other metastatic site which is amenable to future definitive treatment" which can be considered a reasonable baseline definition (25). However, given the wealth of liver directed and systemic therapy options available, it is imperative that each patient with liver predominant disease and therapy is discussed in a multidisciplinary setting. It is also important in clinical practice to evaluate extrahepatic disease, both in terms of its volume relative to liver disease and their rate of progression. The following question can help to frame this evaluation: if the extrahepatic disease is allowed to grow unchecked during the time required for preparation for, delivery and recovery from regional therapy, will this patient ultimately benefit by the proposed course of liver directed treatment? If the answer is yes, then the next step will be selection of the optimal liver-directed therapy. In the setting of cirrhosis, an additional clinical challenge is to judge the severity of the patient's non-oncologic liver disease and estimate the risk of decompensation in comparison to the risk posed by progression of malignant disease. Many HCC patients, in particular, will die of liver failure with malignant disease in check and once again balancing the treatment related toxicity profile with treatment benefit is critical (26).

Radioembolization can be delivered either to an anatomical lobe, cuinard segment (segmental), super-selectively to subsegmental arteries, or to the entire liver. In cases where a tumor is isolated to <2 hepatic segments, it may be possible to deliver an ablative radiation dose to the entire vascular territory (tumor and liver) by infusing only the affected segmental arteries, using TARE or radiation segmentectomy / Lobectomy (RS/L) (27). These segmen-

Please cite this article as: N.K. Sharma *et al.*, The American Brachytherapy Society consensus statement for permanent implant brachytherapy using Yttrium-90 microsphere radioembolization for liver tumors, Brachytherapy, https://doi.org/10.1016/j.brachy.2022.04.004

tal treatments are highly targeted, and frequently deliver higher doses to tumors with decreased toxicity due to the minimal volume of surrounding liver subject to high levels of radioactivity. For this reason, in patients with a small number of tumors (15,14,16), this therapy can be considered focal, and if technically possible may be used as an ablative curative strategy, similar to SABR, radiofrequency ablation (RFA) or transarterial chemoemobilzation (TACE), with the latter two performed by interventional radiologists. A detailed discussion of various focal therapies is beyond the scope of this report, but it is recommended to consider TARE or other focal strategies, if possible, for a patient with a small number of targetable tumors. For those with additional disease that is not focally targetable, an embolic approach remains an appealing way to target tumors with relative sparing of liver parenchyma.

To address the questions above related to liver resection, patients require recent imaging and laboratory studies, including liver function tests. High quality liver imaging is critical and may either take the form of a contrast-enhanced liver CT (ideally with 3 contrast phases) or liver protocol MRI with contrast. This should be complemented by whole body imaging (CT chest/abdomen/pelvis, and optionally, PET-CT or possibly nuclear medicine bone scan) to confirm the extent of extrahepatic disease. Important laboratory tests include serum chemistry with liver enzymes. Particular attention should be given to the total bilirubin, as radioembolization may be unsafe with a level over 2.0 mg/dL, and a trend in this direction should be evaluated carefully in the context of the timing of the procedure. Additional liver enzymes should be reviewed closely as well, and kidney function should be assessed with BUN and creatinine levels to ensure contrast can be safely administered. Complete blood count is important, particularly for patients with hypersplenism and decreased platelets who are a risk of bleeding, and liver synthetic function can also be assessed using coagulation studies. The potential impact of any abnormalities in these tests on the safety of the planned procedure should be carefully considered before progressing. Multi-disciplinary discussion of these issues is critical, and valuable input should be obtained from interventional radiologists, radiation oncologists, surgeons, medical oncologists and hepatologists, as there are many competing risks for these patients that must be considered when defining optimal therapy.

^{90Y} *TARE brachytherapy workflow*

Pretreatment angiogram for microspheres mapping

Pretreatment planning angiography is currently an important step before radioembolization (28). The pretreatment planning angiogram allows for detailed evaluation of the vascular supply to the liver and tumor as well as identifying any non-target vessels that may supply the GI tract. The angiogram and hepatic mapping also allow for the determination of the appropriate location for administration of ^{99m}Tc macroaggregated albumin (MAA) to quantify the lung shunt fraction and assess perfusion within the intended treated volume.

The pretreatment planning angiogram is typically performed via either a common femoral or radial artery access (29). A superior mesenteric angiogram (SMA) is performed to identify variant anatomy to the liver, such as a replaced right hepatic artery, and evaluate the patency of the portal vein. Next a celiac artery angiogram is performed. When performing angiography of the mesenteric vessels a typical rate of about 5 mL/*sec* for a total volume of about 25 mL is used. It is key to make sure that the contrast refluxes into the aorta as variant anatomy can arise extremely proximally off the SMA and celiac artery (Fig. 1). A microcatheter system is used to selectively catheterize the target vessels and angiograms are then performed. It is also important to hold these angiograms out into the portal venous phase as this may be an important clue to the presence of extrahepatic vessels. The use of a high quality pre procedural CT angiogram of the mesenteric vessels before catheterization increases both efficiency and safety of the planning angiogram. Anatomical variants, parasitic vessels and tumor vasculature may be better understood in this manner before the invasive phase of planning begins (30).

The most common extrahepatic vessels identified are the gastroduodenal artery and the right gastric artery (Fig. 2). The easiest way to prevent radioembolic material from going into these vessels is to administer the dose distant to these vessels, although this may not always be possible and coil embolization may be necessary (31–33). It is recommended that new users have a low threshold to perform prophylactic embolization of these extrahepatic vessels when identified. Techniques other than coiling have been used to prevent administration of radioembolic microspheres into extrahepatic vessels, including proximal protection with antireflux devices (34) and splitting the dose to allow administration further away from the extrahepatic vessels. With regards to the falciform artery (Fig. 3), coil embolization may not always be possible, and this can be protected from the effects of radioembolization by placing an ice pack on the patient's abdomen during dose delivery (35,36).

Cone beam CT (CBCT) imaging is strongly recommended, if available, during the pretreatment planning angiogram to help determine vascular supply to the tumor and detect potential extrahepatic vessels. CBCT allows for appropriate vessel targeting and ensures tumors are treated in their entirety, especially in patients undergoing "radiation segmentectomy" (37).

^{99}mTc-MAA is prepared by adding ^{99}mTc-pertechnetate to a kit, however, the tagging is not 100% efficient, with the prepared dosage containing some free ^{99}mTc-pertechnetate. Consequently, patient images after ^{99}mTc-MAA administration may show signal in the common sites of ^{99}mTc-pertechnetate uptake (e.g., thyroid, salivary

Please cite this article as: N.K. Sharma *et al.*, The American Brachytherapy Society consensus statement for permanent implant brachytherapy using Yttrium-90 microsphere radioembolization for liver tumors, Brachytherapy, https://doi.org/10.1016/j.brachy.2022.04.004

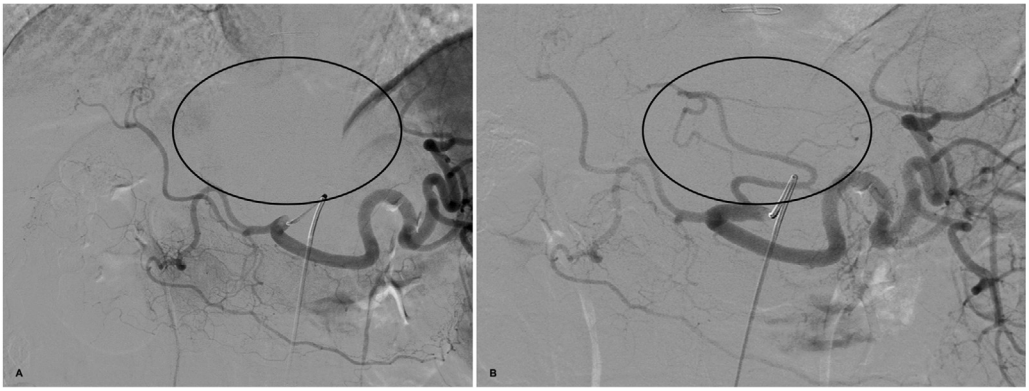

Fig. 1. Angiogram of the celiac artery performed during mapping procedure. (a) shows that the catheter is too far in without reflux of contrast to the aorta demonstrating lack of enhancement of the left lobe of the liver (circle). (b) shows angiogram after repositioning of catheter more proximally within the celiac artery demonstrating a replaced left hepatic artery off the left gastric artery which was initially missed on the earlier angiogram.

Fig. 2. Common hepatic angiogram shows the gastroduodenal artery (black arrow) and the right gastric artery (white arrow).

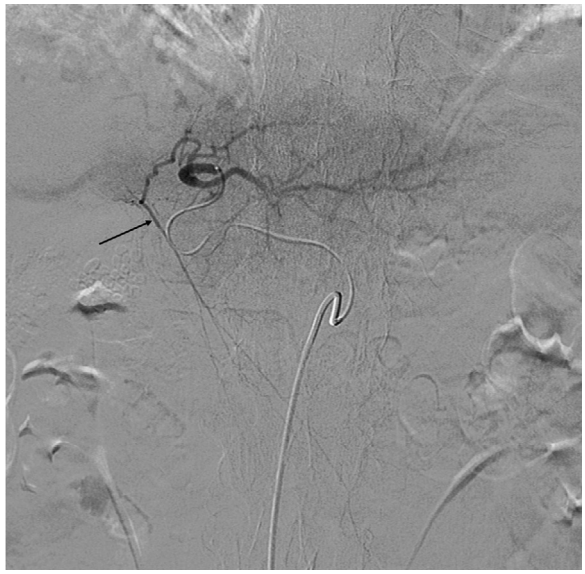

Fig. 3. Left hepatic artery angiogram demonstrates filling of the falciform artery off a branch to segment 4 (black arrow).

glands, and renal cortex). ^{99}mTc has a physical half-life of 6.01 h whereas elimination of ^{99}mTc-MAA from the human lungs has been reported to occur with an effective half-life of 3.8 h. It is typical to complete imaging of patient in the first 2 h of ^{99}mTc-MAA administration and therefore mitigate any complication arising for *in vivo* degradation of ^{99}mTc-MAA.

Once the target vessels are identified, approximately 5mCi of^{99m}Tc-MAA is typically injected via the microcatheter into the main trunk of the target vessels (e.g., right hepatic artery or left hepatic artery). In cases where there is bilobar disease, ^{99m}Tc-MAA can be split into the right and left hepatic arteries (2.5 mCi into each branch), 2 doses of ^{99m}Tc-MAA can be given one into each artery, or the ^{99m}Tc-MAA can be delivered into the lobe with the highest burden of disease per physician discretion.

All catheters are then removed, and the patient's arterial access is sealed before being sent to the NM clinic for the lung shunt study which can be done as planar images or single photon emission computed tomography/computed tomography (SPECT/CT) imaging. These images always include the chest and abdomen to visualize the distribution of ^{99m}Tc-MAA. It is important to note that the distribution within the liver may not reliably predict the distribution of ^{90}Y, due to differences in catheter location, flow dynamics, or presence of proximal bifurcations among other factors. Nonetheless, it can be helpful in identifying any missed enteric branches or falciform artery. (38–40)

Determination of the lung shunt fraction and the mean lung dose

Several publications have shown that the ^{99m}Tc MAA planar imaging overestimates the lung shunt fraction (LSF)

Please cite this article as: N.K. Sharma *et al.*, The American Brachytherapy Society consensus statement for permanent implant brachytherapy using Yttrium-90 microsphere radioembolization for liver tumors, Brachytherapy, https://doi.org/10.1016/j.brachy.2022.04.004

relative to ^{99m}Tc MAA SPECT/CT (41–46). Overestimates may be due to MAA breakdown, scatter and attenuation differences between liver and lung, and using both geometric mean of liver (more attenuating through posterior view, so lower counts → overestimate). One study found no significant difference between ^{99m}Tc-MAA SPECT/CT and post-therapy ^{90}Y PET/CT imaging (44), whereas another reported absolute lung shunt differences (47) on the order of 4%, with MAA being larger (6% vs. 2%). Lung masses in a relatively small population ranged from −25% to +64% of the nominal 1 kg lung mass (48,46); this would have direct impact on organ-level MIRD lung dosimetry (see dosimetry section below). In addition, segmentation of lung on free breathing CT would lead to additional variability on the order of 15%.

MAA is known to be an imperfect surrogate for both glass and resin microspheres. It has a different size, shape, density, and the number of particles administered is significantly less. It also degrades over time; thus, it is important to scan quickly or free pertechnetate can be seen on the scan. MAA spans a wide range of sizes, with 90% between 10 and 70 μm, and smaller particles shunting more easily. Even if 99mTc-MAA were a perfect surrogate for ^{90}Y microspheres, respiratory motion, spatial resolution (spill-out of counts from liver into lung), attenuation & scattering differences between lung and liver, segmentation of lung and liver, and their conversion to mass still play a role in the precision and accuracy of LSF and eventual lung dose (46). Attenuation and scatter correction can be accomplished with ^{99m}TcMAA SPECT/CT, but mismatch with the attenuation scan can lead to additional biases. Furthermore, lung dose estimated from post-therapy ^{90}Y PET/CT may be undetectable and susceptible to noise given the low positron yield of ^{90}Y and low activity expected in the lungs.

In current practice, the lung dose rarely limits the activity to administer. A recent simulation study has shown that respiratory motion has minimal effect on LSF (49). When transitioning to voxel-level dosimetry, it will be important to have a local density scaling in the local deposition method (LDM) or kernel methods when calculating lung doses, as differences were reported to be 60% lower when using a single density value for the dose calculation (50).

Vendor provided package insert estimation of lung dose limits based on planar imaging with fixed 1 kg lung mass may not be appropriate when used with SPECT/CT based estimates. Dose limits would need to be reassessed by investigating reported SPECT/CT LSF and lung doses when using SPECT/CT for lung dose to refine or update current limits.

A recent publication reviewed the various methods of determining the LSF and lung mean dose (LD), encompassing pretherapy and post-therapy assessments of the LSF and LD using both 2D planar and 3D SPEC T/CT based calculations (51). The authors present a lexicon to precisely describe the methodology used for the estimation of LSF and LD; specifically, category, agent, modality, contour and algorithm, to aid in their interpretation and standardization in routine clinical practice.

Both SIR-Spheres and TheraSphere package inserts define 30 Gy and 50 Gy as lung mean dose limits for single and cumulative radioembolization treatments, respectively; SIR-Spheres instructions for use pamphlet (IFU) imposes an additional LSF maximum limit at 20%. A recent review article summarized the historical context and literature for origins of the current lung dose limits after radioembolization along with newer clinical evidence based on larger patient cohorts that challenge the historical data on lung dose limits. The authors conclude by proposing a staged approach to advance the field of lung dosimetry (52).

Equations for lung shunt fraction (LSF) and lung dose calculation are described next.

$$LSF = \frac{(Lung\ Counts)}{(Lung\ Counts)\ + (Liver\ Counts)}$$

where *Lung Counts* and *Liver Counts* are the ^{99m}Tc-MAA counts (or activity) in the lung and liver regions/volumes of interest in ^{99m}Tc-MAA images. The net ^{90}Y activity expected in the lungs, A_{lung}, can be determined as:

$$A_{lung}[GBq] = A_{admin}\ [GBq]\ \times\ LSF$$

where A_{admin} is the net ^{90}Y administered activity for the therapy. The resultant mean dose to the lung can be determined as:

$$Lung\ Dose\ [Gy] = 50\left[\frac{Gy \cdot kg}{GBq}\right] \times LSF \times A_{admin}[GBq] \times \frac{1}{M_{lung}[kg]}$$

where M_{lung} is the estimated lung mass.

The maximum activity, A_{max}, that can be implanted in a patient with a given LSF and M_{lung}, that delivers a limiting lung dose of 30 Gy, can be described as:

$$A_{max}\ [GBq] = 30\ [Gy] \times M_{lung}[kg] \times \frac{1}{LSF} \times \frac{1}{50\left[\frac{Gy \cdot kg}{GBq}\right]}$$

Tumor burden determination

Qualitative estimates of tumor burden are often performed with 3D segmentation on anatomical imaging most often using contrast-enhanced CT or MRI diagnostic imaging. Supplemental imaging modalities such as intra-arterial contrast enhanced cone-beam CT, or CT angiography, or ^{99m}Tc-MAA SPECT/CT may also be used. Estimating tumor burden can be difficult for infiltrative/diffuse disease. And most current estimates of tumor burden ignore functional aspects. Perfused liver and tumor volumes based on ^{99m}Tc-MAA SPECT/CT that are fused with diagnostic images are also valuable in identification of tumor voxels. Some recent works have proposed segmentation of the normal liver using SPECT/CT of liver functional imaging

Please cite this article as: N.K. Sharma *et al.*, The American Brachytherapy Society consensus statement for permanent implant brachytherapy using Yttrium-90 microsphere radioembolization for liver tumors, Brachytherapy, https://doi.org/10.1016/j.brachy.2022.04.004

agent (e.g., sulfur colloids, or IDA agents), which would aid in separating normal liver parenchyma from tumor in the liver leading to more accurate tumor burden estimates (53,54).

Dosimetry

The amount of radioactivity administered, in addition to the intended target volume, and microsphere distribution within the target volume largely dictate the magnitude and effect of the resulting radiation dose delivered. Inherent to this process is a variability in the distribution of radiation that cannot reach the same degree of targeting as external beam radiation techniques. However, radioembolization allows for the treatment of vascular anatomical segments, and multi-centric lesions that cannot be safely or effectively treated by external beam radiotherapy (55). Conceptually, TARE can be considered a type of intra-arterial brachytherapy, with radioactive microspheres of sizes between 20 and 60 μm that number in the millions. Controversy still exists as to both predictive and post-implantation activity recovery, and dose/microsphere distribution in current commercially available products (56). Future iterations of TARE may include radiopacity that allow for real time tracking of radiation implantation and reliable post procedural imaging that would improve on the predictive and quantitative analysis of administered dose (57).

Due to the variability of the specific activity per particle (through modulation of the decay from time of calibration, or inherent to the specific commercial product), various dosimetric techniques for conventional therapy (i.e., optimization of radiation to tumor and minimization of parenchymal exposure) have been proposed and implemented. A discussion relating to the differences with respect to characteristics, activity and delivery of the currently available commercial products is beyond the scope of this document and well-described in other publications (58). The most common activity calculation methods consist of the single-compartment Medical Internal Radiation Dose (MIRD) model, the three compartment Partition Model (PM, consisting of the lung, liver and tumor), the Body Surface Area (BSA), and the voxel dosimetry model. Although the so-termed Empiric model has been reported, this dosimetry approach has been largely abandoned and no longer part of the package insert for SIR-Spheres. A brief overview of the activity or dosimetry determination models will follow.

Method 1: Body surface area (BSA)

The Body Surface Area (BSA) method (59) is an activity prescription method. It accounts for a theoretical liver volume based on an individual's BSA (i.e., height and weight), supplemented by the tumor involvement in the liver (TI is the ratio of volume of tumor to the volume of tumor and normal liver). It is applied with resin microspheres and the activity for administration is determined utilizing the following equation:

$$A[GBq] = (BSA\ [m^2] - 0.2) + TI$$

Where

$$BSA[m^2] = 0.2025 \times height[m]^{0.725} \times wieght[kg]^{0.425}$$

The dependence on the linear relationship between body surface area and liver volume represents a significant concern, for unlike pharmacological distribution of systemic therapy, increased weight (i.e. obesity) does not alter the actual volume of liver, and the often associated fatty liver may in fact contribute to an increased risk of hepatotoxicity (60). This model is used as part of the package insert dosimetry for SIR-Spheres.

Method 2: Partition model (PM)

The partition model (PM) represents a more accurate method of determining the amount of activity required to achieve the desired target dose (61). Consisting of two compartments, the model allows for the estimation of target dose to normal liver parenchyma, and the tumor compartment. These calculations are determined through a combination of the ratio of microsphere uptake in the tumor compartment compared to the normal liver, and the individual volumes of the tumor and normal liver compartments in the targeted area. Although the volumes of the tumor and of the normal liver are determined from anatomical images (see prior section), the ratio of microsphere uptake for the tumor compartment compared to the normal liver (TNR), as shown below, is determined as MAA counts per unit volume (or per unit mass) of the compartments based on ^{99m}Tc-MAA SPECT/CT.

$$TNR = \frac{Tumor\ Uptake\ [MAA\ counts]/Tumor\ Volume\ [ml]}{Normal\ Liver\ Uptake\ [MAA\ counts]/Normal\ Liver\ Volume\ [ml]}$$

The total activity in volume that can be associated with the tumor and normal liver compartments can be calculated as follows:

$$A_{tumor}[GBq] = A_{admin}[GBq] \times \frac{(1 - LSF) \times TNR \times M_{tumor}[kg]}{M_{normal\ liver}[kg] + M_{tumor}[kg] \times TNR}$$

$$A_{normal\ liver}[GBq] = A_{admin}[GBq] \times \frac{(1 - LSF) \times M_{normal\ liver}[kg]}{M_{normal\ liver}[kg] + M_{tumor}[kg] \times TNR}$$

where, A_{tumor} and $A_{normal\ liver}$ are the activity or counts in tumor and normal liver compartments, whereas M_{tumor} and $M_{normal\ liver}$ are the mass of tumor and normal liver compartments, respectively. The radiation absorbed dose to each of the two compartments, tumor(s) and normal liver, can be determined by inserting the corresponding activity and mass for that compartment into the dose equation

Please cite this article as: N.K. Sharma *et al.*, The American Brachytherapy Society consensus statement for permanent implant brachytherapy using Yttrium-90 microsphere radioembolization for liver tumors, Brachytherapy, https://doi.org/10.1016/j.brachy.2022.04.004

below:

$$Dose_{compartment}\left[Gy\right] = 50\left[\frac{Gy\cdot kg}{GBq}\right]\times\frac{A_{compartment}\left[GBq\right]}{M_{compartment}\left[kg\right]}$$

Method 3: MIRD

The MIRD method is a well-known dosimetric technique that accounts for the volume of the target tissue and reports only the mean absorbed dose to tissue irrespective of the differential distribution of microspheres in the tumor versus the normal parenchyma. The absorbed dose delivered is based on energy released per disintegration under equilibrium conditions of uniform microsphere distribution and energy absorption in volume (61). The volume element must be large enough such that partial volume and edge-effects of dose deposition can be disregarded, and, furthermore, it ignores the microscopic variation in dose distribution. This may represent a gross oversimplification of the dose distribution, as radioactive microsphere distribution within the volume (i.e., tumor vs. liver) is not taken into account. Only the mean dose is reported as follows. This model is used as part of the package insert dosimetry for Therasphere glass microspheres.

$$Dose_{volume}\left[Gy\right] = 50\left[\frac{Gy\cdot kg}{GBq}\right]\times\frac{A_{volume}\left[GBq\right]}{M_{volume}\left[kg\right]}$$

Method 4: Voxel-based dose calculation

The dosimetry models described previously were either empirical or MIRD style organ dosimetry that reported mean dose to perfused volumes. More recently radiation transport methods such as Monte Carlo simulation, local deposition, and dose-kernel methods such as dose-voxel kernels (DVK), voxel-S-values (VSV), dose-point kernels (DPK), and convolution-superposition (62–67) have been used to estimate the absorbed doses for ^{90}Y-radioembolization at the voxel level. These are the computational gold standard, given accurate cross sections, decay data, and true spatial distributions of the activity, material, and density distribution. These so-called voxel dosimetry approaches have been used for both post-therapy imaging and retrospective MAA-based dosimetry (68–70,50,71,72). Local deposition is an approach that assumes all energy emitted by the radionuclide is absorbed locally within the voxel it originated from and takes advantage of the large voxel sizes present in NM imaging modalities. The liver is a largely homogeneous organ and all voxel-based calculations agree to within $\approx 5\%$ in soft tissue (50,49).

Similar to the PM, voxel-level dosimetry requires an emission and anatomic scan to perform a single time point dose rate calculation. Assuming no biological clearance, the dose rate map is transformed to an absorbed dose map. These dosimetry models may be applied to planning ^{99m}TcMAA SPECT/CT images, post-therapy ^{90}Y bremsstrahlung SPECT/CT or ^{90}Y PET/CT images (Fig. 4). As the dosimetry model relies upon the activity distribution determined from imaging, therefore, limitations and inaccuracies in the imaging input will directly affect the absorbed doses reported.

Given the current spatial resolution of PET/CT and SPECT/CT, there is little reason to pursue voxel-level full radiation transport in the liver due to the average projected range of the beta being less than or equal to the spatial resolution of reconstructed ^{99m}TcMAA SPECT, ^{90}Y SPECT, or ^{90}Y PET. However, transport may still prove useful in the lung and at the liver/lung interface due to the betas traveling 4 times farther due to lower density lung compared to liver (50,49).

$$D_{i,j,k}\left[Gy\right] = 50\left[\frac{Gy\cdot kg}{GBq}\right]\times\frac{A_{i,j,k}\left[GBq\right]}{M_{i,j,k}\left[kg\right]}$$

Where $D_{i,j,k}$, $A_{i,j,k}$, and $M_{i,j,k}$ corresponds to the dose, activity, and mass of voxel (i,j,k), respectively.

^{90Y} Microsphere delivery

During the dose administration the microcatheter is placed into the target vessel as done during the mapping procedure. Many of the angiograms are repeated to make sure there are no new extrahepatic vessels that have arisen or recanalization of previously embolized vessels (68,69). The selected radioembolic particles are then injected through a microcatheter into the target vessels under fluoroscopic guidance. Radioembolic material should not be injected through a diagnostic catheter. Once the dose is administered the microcatheter is removed slowly from the base diagnostic catheter and the tip captured in a 4×4 inch piece of gauze as to prevent unintended splattering of radiation dose that may be residual within the microcatheter. The microcatheter is then placed inside a Nalgene jar with delivery apparatus and placed in radioactive waste storage to decay as per institutional policy (64,65) . After hemostasis is achieved from the vascular access the patient is sent for post-^{90}Y scan and then discharged home.

Post therapy evaluation with bremsstrahlung spect or PET

Post-therapy imaging can serve different purposes: (*1*) qualitative verification that the spatial deposition of the ^{90}Y microspheres is consistent with the planned delivery and written directive, (*2*) verification of the total activity administered, (*3*) semi-quantitative activity distribution that can be used to estimate the absorbed dose to lesions and non-tumoral liver. This can be especially helpful if further radiation-based treatment is needed with radioembolization or external beam radiation therapy. Qualitative verifications can be performed with either the post-therapy ^{90}Y PET/CT (Fig. 4) or ^{90}Y SPECT/CT distribution compared to the

Please cite this article as: N.K. Sharma *et al.*, The American Brachytherapy Society consensus statement for permanent implant brachytherapy using Yttrium-90 microsphere radioembolization for liver tumors, Brachytherapy, https://doi.org/10.1016/j.brachy.2022.04.004

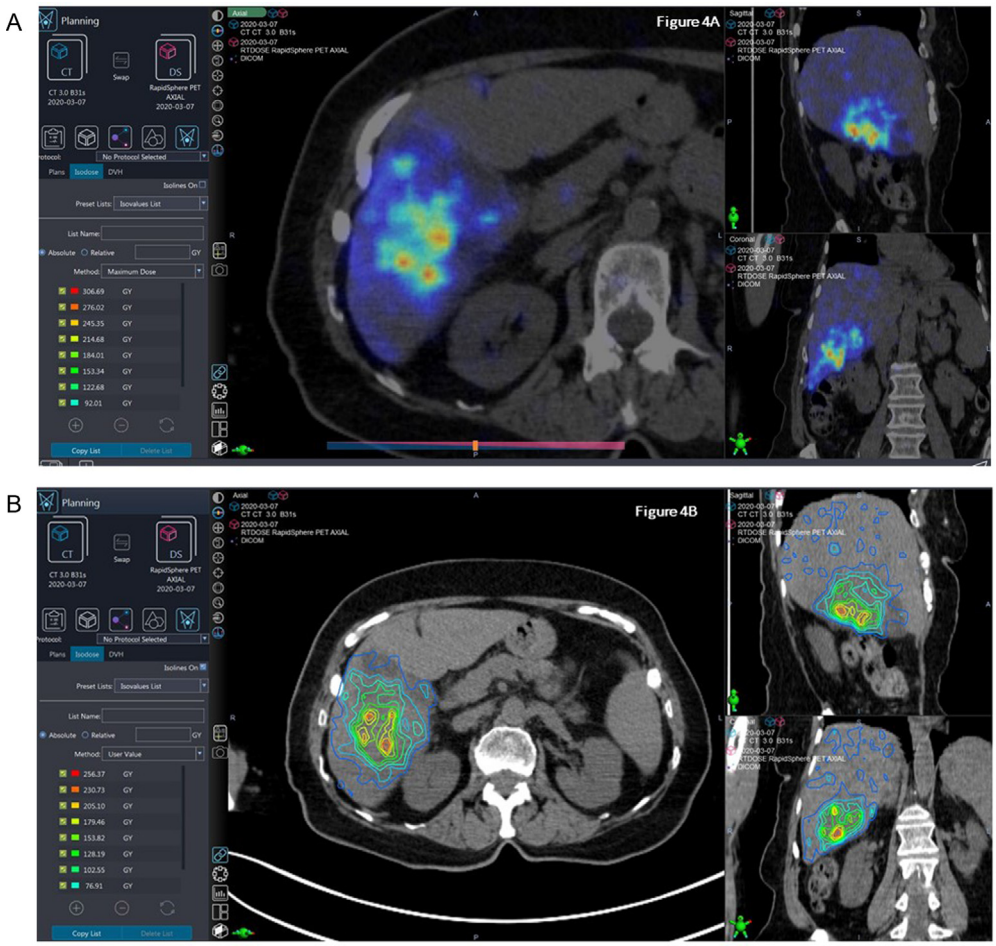

Fig. 4. Using post ^{90}Y PET/CT dosimetry to calculate radiation dose distribution in a 67 yo patient with metastatic colon cancer treated to the right lobe with 34 mCi ^{90}Y resin microspheres. Fig. 4a: Post-^{90}Y treatment PET/CT acquisition demonstrating high dose distribution in targeted areas. Fig. 4b: Isodose line representation of dose distribution.

pre-treatment ^{99}mTc MAA SPECT/CT or CTA performed during the mapping procedure.

Respiratory motion is known to degrade quantitative accuracy of emission scans. A simulation study of ^{90}Y PET/CT showed that on average the breathing motion decreased activity recovery depending on the tumor size and magnitude of respiratory motion (49). Overall, the net accuracy of the post-therapy ^{90}Y quantitation depends on a number of factors including image noise, acquisition mode, respiratory motion, and the reconstruction parameters used in construction of ^{90}Y SPECT/CT and ^{90}Y PET/CT images (73,74).

Regarding quantification of image-based total activity administered, for a given reconstruction method and population of patients, both clinical PET and SPECT reconstructions are imperfect with counts placed outside the liver or known phantom filled with ^{90}Y concentrations. Because of this, several groups have pursued the use of self-calibration (50,75). Self-calibration can be used for both post-therapy ^{90}Y PET/CT and SPECT/CT. A calibration factor can be determined for a set number of patients and then used going forward.

In theory, self-calibration would not be needed if image reconstruction were perfect. Quantification of the total activity administered can be performed by measuring the total activity in the field of view on PET/CT and/or applying a previously measured calibration factor (i.e., sensitivity factor cps/mL->Bq/mL) for SPECT. Verification of the quantitative accuracy of integrating the field of view or the liver contour should be tested in phantom studies, as there can be large differences (up to 70%) between the FOV and liver VOI calibration (76).

^{90}Y microsphere PET/CT is feasible given the low positron yield of 32 ppm (77,78) and high energy bremsstrahlung incident on the detector (79). The QUEST study also reported scanner quantitative accuracy over several different manufacturers and models for different reconstructions (80). A phantom study showed that ^{90}Y PET/CT dosimetry was within 10% of expected for spherical lesions $>$ 10 cc (81).

Please cite this article as: N.K. Sharma *et al.*, The American Brachytherapy Society consensus statement for permanent implant brachytherapy using Yttrium-90 microsphere radioembolization for liver tumors, Brachytherapy, https://doi.org/10.1016/j.brachy.2022.04.004

Our understanding of the limitations in ^{90}Y PET/CT due to the low positron yield continues to evolve. Thus, optimization of the number of bed positions or the location of liver or tumor within a single bed position, or the use of continuous bed motion are still areas of research being explored (82). When designing scanning protocols for ^{90}Y PET, the low positron yield and activity administered must be accounted for to optimize quality of decay capture (82,83,74). Respiratory motion compensation also plays a role in the emission imaging, especially at the dome of the liver where motion during respiration can be > 2 cm (73). Respiratory motion will impact PET more so than SPECT due to the difference in spatial resolution of the modalities.

Although ^{90}Y bremsstrahlung SPECT/CT has worse spatial resolution compared to PET, it is still useful for verifying the delivered distribution is in the correct anatomic location. In addition, there are varying degrees of quantitative SPECT that can be performed. One group used a background compensation method (84) whereas others have taken more sophisticated steps to model the high energy bremsstrahlung, scatter, and attenuation in the patient, collimator, and detector (85–88). ^{90}Y SPECT/CT imaging is performed with parallel hole collimator designed for either medium-energy or high-energy gamma emissions.

A number of commercial software solutions exist to pursue voxel-level absorbed doses on post-therapy scans. These typically employ a local energy deposition or voxel-S value kernel as described in MIRD report 17 (62). When used for post-therapy dosimetry, particular attention should be paid to the calibration-factor that converts counts rate to activity. Both SPECT and PET reconstructions are imperfect, and choosing a self-calibration based on the liver volume, perfused liver volume, or entire field of view can lead to substantially different results.

The use of 3-dimensional (3D) dose distribution based on ^{90}Y PET imaging provides an improved understanding of radiation dose distribution (89). Another method using time of flight (TOF) PET scan increases tumor visibility of microsphere deposition in the liver and permits the quantification of the total activity delivered to the liver during radioembolization (90). Digital PET/CT also provides image quality and ^{90}Y to background contrast as compared with Bremsstrahlung SPECT/CT (91). Given the limitations in the ability to correctly predict final ^{90}Y activity distribution using ^{99}Tc-MAA, methods to incorporate ^{90}Y PET scan and the importance of catheter positioning can optimize patient-specific treatment planning, efficacy and safety based on pretreatment imaging (52). Likewise, PET/Magnetic resonance imaging (MRI) demonstrates comparable dosimetry values compared to PET/CT (92). Therefore, PET-based scanning before and after radioembolization seems to be superior with respect to its ability to forecast dose distributions and inform the physician as to how to safely prescribe dose.

Radiation safety considerations

^{90}Y is a pure beta emitter with a maximum energy of 2.28 MeV, average energy of 0.93 MeV, and half-life of 64.1 h (93). As part of a radiation safety program, the authorized user and radiation safety officer must take the safety of the patient, staff, and general public into consideration.

^{90}Y beta particles are relatively easy to stop with a little in excess of 1 cm water-equivalent material (e.g., acrylic). However, this does give rise to bremsstrahlung x-rays which are then typically shielded by a lead container holding the vial with microspheres. Glass microsphere (GMS) administration takes place with the vial in an acrylic shield that sits in a lead pig enclosed in a plastic beta shielding box, whereas resin microspheres are in a v-vial enclosed in a plastic beta shield box. The administration kits do stop the beta particles; however, the betas can stream through the air when traveling through the tubing and catheter located outside the administration kit before entering the patient. The mean and maximum range of ^{90}Y beta particles in air is ~4 m and ~10 m, respectively (4).

Absorbent coverings should be placed on the floor of the interventional radiology suite before the procedure. Staff involved in the procedure must wear protective equipment including lead-equivalent aprons, double gloves, gown, face mask, and double shoe covers. Everyone leaving the room after administration is scanned to make sure they are not contaminated before being allowed to exit. All contaminated items must be collected and disposed of as radioactive waste. A survey after the procedure is required to ensure no contamination is left in the room including trash and personnel.

Surveying physicians after administration can be difficult due to close patient proximity, which causes an increase in background radiation. Increasing the distance from the patient and using the lead-equivalent aprons of the physician and surveyor as shields can help lower the background radiation originating from the patient, which will aid in detecting small amounts of contamination.

Radioactive materials are subject to statutes and regulations regarding their receipt, storage, handling, use, and disposal. Studies have estimated exposure rate constants for ^{90}Y bremsstrahlung to help determine administered activities that may result in public exposure limits (94,95) being exceeded. Gulec and Siegel estimated that 9 GBq administered could result in 1 mSv being received by the most exposed person. Instructions should also be provided to the patient to minimize exposure to others. In addition, a letter could be given to the patient if they are traveling that describes the medical administration of radioactive materials to explain triggering of radiation detectors at airports or border crossings. More detailed regulatory issues have been discussed elsewhere (96,97,8,6,98). Nevertheless, all users and facilities must abide by their local, state, and federal regulations.

Please cite this article as: N.K. Sharma *et al.*, The American Brachytherapy Society consensus statement for permanent implant brachytherapy using Yttrium-90 microsphere radioembolization for liver tumors, Brachytherapy, https://doi.org/10.1016/j.brachy.2022.04.004

Nuclear medicine clinical equipment considerations

Clinical support of ^{90}Y TARE, specifically by a medical physicist, involves a variety of equipment that are typically present in clinical nuclear medicine (NM) departments. They include non-imaging equipment such as dose calibrators, Geiger-Muller (GM) survey meters, ionization survey meters, as well as imaging equipment such as gamma camera, SPECT/CT, and PET/CT systems. We now briefly discuss the some of the salient features and the appropriate use and setup for some of this equipment. Additional information on these and associated topics can be found in various nuclear medicine textbooks and review articles. (98)

Dose calibrators

The dose calibrator is a critical piece of equipment because it is used to determine the ^{90}Y activity planned for delivery. Recall that ^{90}Y decay does not have an associated photon emission, consequently, the photons detected by the dose calibrator to estimate the ^{90}Y activity are the secondary bremsstrahlung photons from the energetic beta emission. Because the carrier material and form factors for the dispensed activity are different between the two approved devices, the efficiency of bremsstrahlung signal production may be different leading to different calibration numbers for dose calibrator when measuring ^{90}Y activity. Consequently, it is imperative to calibrate the dose calibrator separately for each ^{90}Y device. This is done by requesting (typically three) calibrated ^{90}Y activity vials (with accuracy better than 5%) from each of the vendors to adjust the dose calibrator setting. It is also important to note that the accuracy of the dose calibrator may also be sensitive to the volume of ^{90}Y microspheres present in the vial, but this is a second order effect, and more relevant during preparation of the ^{90}Y microsphere activity for administration. (98)

GM survey meters

The GM survey meter is used to identify any ^{90}Y contamination in the area used for preparation of the activity for dispensation (such as a hood in NM hot laboratory) or after delivery of the ^{90}Y microspheres in the IR suite. Care must be taken to use the GM meter with the beta (plastic) cover removed from the face of the GM detector so that the beta emission from ^{90}Y decay can be readily detected (else they will be absorbed and stopped by the plastic shield). Furthermore, area monitoring with GM survey meter must be done slowly to allow time for the GM tube to respond to presence of energetic beta that may be detected.

Ionization survey meters

The ionization survey meter is typically used to determine the exposure rate. However, patient exposure rates are not a concern, and therefore not measured routinely, as stated in the section on Radiation Safety consideration. The main use of an ionization survey meter in support of ^{90}Y TARE is for the determination of the net administered activity as follows: the exposure rate of the administration vial is recorded at a known distance (typically 30 cm). The exposure rate of the radioactive waste (activity vial, administration tubing, catheters, etc.) placed in a plastic jar which is, in turn, enclosed in an acrylic cylinder, is also measured. The ratio of the decay-corrected waste jar exposure rate to the administration vial exposure rate provides an estimate of the residual waste fraction. The residual waste fraction is needed to determine the net administered ^{90}Y activity. Knowledge of the net administered activity is a fundamental measurement that forms the basis of radiation dosimetry. Therefore, it is essential that the ionization meter used is calibrated and that the exposure measurements are acquired consistently. (98)

Gamma cameras

A gamma camera is used for assessing the *in vivo* 2D-biodistribution of radioactivity. The clinical value of ^{99}mTc-MAA planar biodistribution assessment is primarily for lung shunt calculation and identification of unexpected extra-hepatic deposition as previously described in sections *Pretreatment Angiogram for Microspheres Mapping and Determination of the lung shunt fraction and the mean lung dose.* In terms of the ^{99}mTc imaging protocol, we recommend the use a photopeak energy window centered at 140 keV and width of 15% (or 20%) with low-energy collimation. The gamma camera scintigraphy could be acquired either as static images or whole-body scans. Planar scintigraphy does not typically use scatter compensation, though it may be applied if desired. (99)

The clinical value of ^{90}Y-microsphere planar biodistribution assessment is to verify that the ^{90}Y microspheres are localized to the liver (SPECT is strongly recommended over planar imaging). Due to the nature of scintigraphy (overlapping organs and lack of anatomical delineation), ^{90}Y-microsphere planar images cannot adequately distinguish between tumors and normal liver tissue. Although there are no standardized energy windows or collimators for ^{90}Y radionuclide, an imaging energy window 90–125 keV and medium-energy collimation have been shown to produce adequate ^{90}Y scintigraphy. (84)

SPECT/CT scanners

A SPECT/CT system is used for assessing the *in vivo* 3D-biodistribution of ^{90}Y radioactivity along with the corresponding anatomical imaging provided by the CT scanner. The advantage of SPECT/CT over planar imaging is the ability to generate a more accurate representation of the biodistribution due to the corrections for scatter, attenuation, and resolution. Furthermore, SPECT/CT imaging is

Please cite this article as: N.K. Sharma *et al.*, The American Brachytherapy Society consensus statement for permanent implant brachytherapy using Yttrium-90 microsphere radioembolization for liver tumors, Brachytherapy, https://doi.org/10.1016/j.brachy.2022.04.004

often reimbursed when imaging for ^{99}mTc-MAA and ^{90}Y microspheres. ^{99}mTc-MAA SPECT/CT is often used to assess lung uptake and the tumor and normal liver uptake to guide dosimetry-based treatment planning as previously described in sections *Pretreatment Angiogram for Microspheres Mapping and Determination of the lung shunt fraction and the mean lung dose.*

In terms of the ^{90}Y SPECT/CT imaging protocol, there are no standardized energy windows or collimators. There are several review articles that describe ^{90}Y SPECT/CT. A practical ^{90}Y imaging protocol that can be applied to all clinical SPECT/CT systems is using an imaging energy window 90–125 keV and medium-energy collimation with a 310–410 keV scatter compensation window, 120 views over 360° for about 20–30 s per view. Images are reconstructed with iterative reconstruction algorithm that uses CT-based attenuation and energy-window based scatter corrections. (84)

The CT acquisitions as part of SPECT/CT, whereas often a low-dose scan, will benefit from higher image quality (CTDIvol ~ 15 mGy) because improved soft-tissue CT contrast is of clinical benefit for liver and tumor segmentation.

Quantification of absorbed doses after ^{90}Y SPECT/CT is certainly feasible and several review articles have reported on approaches and clinical value. ^{90}Y SPECT/CT is reimbursable and its application for post-treatment dose verification is increasing. In fact, an ongoing multi center prospective clinical trial (NCT04736121) allows for retreatment if radiation doses delivered to tumors were determined to be inadequate based on post-radioembolization ^{90}Y SPECT/CT (100).

PET/CT scanners

A PET/CT system is primarily used for assessing dosimetry post ^{90}Y radioembolization. Although PET/CT may provide quantitative images care must be taken to ensure that ^{90}Y radionuclide is programmed into the PET scanner correctly with the right half-life and positron branching ratio. Due to the low positron branching ratio, ^{90}Y images are acquired for 15–20 min per bed. Furthermore, reconstruction parameters for use with ^{90}Y PET have not been firmly established and care must be taken to ensure the images have converged and issues related to spurious noise signal has been accommodated. PET images are converted to dose using DVK or other dose-kernel based methods. (73,74)

Discussion

Clinical consideration of ^{90}Y TARE and treatment approaches

^{90}Y TARE is a well-established brachytherapy method in the treatment algorithm for unresectable liver cancer. Although ^{90}Y has traditionally been used in advanced disease, application in earlier and intermediate stage HCC has also shown favorable results. There are ongoing refinements in planning and therapeutic technique, especially in areas related to dosimetry and dose response. This ABS consensus report summarizes the current clinical data for both glass (Theraspheres) (101) and resin (SIR-Spheres) (102) microspheres, respectively, and recommends best practices for clinical users.

Radiation segmentectomy considerations

In brief, the radiation segmentectomy / lobectomy (RS/L) technique increases the overall amount of radiation/microsphere delivery such that supra- therapeutic dose of radioactivity is administered to anatomically definable areas of the liver with limited tumor burden, with the additional intent of inducing radionecrosis in the normal liver parenchyma in the treatment angiosome/volume [40, 46]. A comparison of the techniques is outlined for both high and low specific activity scenarios. (Table 2)

Prior embolization

The principle of TARE relies on the ability to exploit the recruitment of neovasculature arising from the hepatic arteries into the tumor. As a result, a vascular conduit must exist, and should be clearly demonstrated through multiphasic imaging (CT or MRI) and confirmed angiographically, with supportive findings on ^{99m}TcMAA injection. Issues such as density of stroma, vascular damage/spasm due to chemotherapy or technique, and intratumoral interstitial pressure may impact the ability to deliver TARE in a target dosimetric range and are inherently evaluated as part of the pre-administration/treatment mapping angiogram. Previous hepatic arterial embolotherapy (bland, lipiodol based chemoembolization, drug eluting bead embolization) anecdotally decreases tumor vascularity and radiographic response. Controversy exists regarding the appropriate sequence of TARE versus conventional embolic therapy.

Combination with other radiation treatments

The knowledge of ^{90}Y dose distribution, tumor location and non-involved liver dose can inform other decisions about re-treatment of a liver tumor using ^{90}Y or external beam RT (EBRT). For example, in a retrospective analysis of 31 patients who underwent ^{90}Y radioembolization after previous external beam radiation therapy, investigators reported that the fraction of liver exposed to ≥30 Gy (V_{30}) was the strongest predictor of hepatotoxicity, and patients with V_{30} >13% uniformly experienced hepatotoxicity (103). Fatal REILD ($n=2$) occurred at the 2 highest EBRT mean liver doses (20.9 Gy and 23.1 Gy) but also at the highest cumulative liver doses (91.8 Gy and 149 Gy).

Please cite this article as: N.K. Sharma *et al.*, The American Brachytherapy Society consensus statement for permanent implant brachytherapy using Yttrium-90 microsphere radioembolization for liver tumors, Brachytherapy, https://doi.org/10.1016/j.brachy.2022.04.004

Table 2
Recommended dose ranges for glass and resin ^{90}Y utilizing conventional RS/L and TARE techniques

	RS/L target	Conventional TARE target
Glass ^{90}Y microspheres (99)	330–400 Gy single-compartment average dose to treated volume	120–150 Gy single-compartment average dose to treated volume
Resin ^{90}Y microspheres (100)	150–200 Gy single-compartment average dose to treated volume	100–120 Gy Partition Model dose to Tumor

MIRD = Medical Internal Radiation Dose; RS/L = radiation segmentectomy/lobectomy; TARE = transarterial radioembolization.

However, this study did not specifically employ ^{90}Y PET scan to guide decision making in EBRT dose delivery. A study of Child Pugh A/B patients treated with radioembolization in Taiwan suggested that the V_{100} (The fraction of normal liver exposed to more than 100 Gy) to V_{140} significantly differed between patients who did or did not experience hepatotoxicity (104). The V_{110} was the strongest predictor of hepatotoxicity. In summary, combined EBRT and ^{90}Y has an acceptable safety profile in appropriately selected patients with the goal to spare previously treated liver using PET based ^{90}Y imaging (to identify untreated liver that may be able to tolerate additional therapy safely).

Selection of patients for ^{90}Y TARE versus HDR interstitial brachytherapy

As not all patients are ideal for ^{90}Y TARE, an alternative treatment option is interstitial brachytherapy, generally using an ^{192}Ir high-dose-rate (HDR) source and CT and/or ultrasound-based needle guidance. This technique was initially tested by Dritschilo *et al.* in the 1980′s, with a dose escalation study reaching single fraction doses of 50 Gy under ultrasound guidance (105). Percutaneous CT-guided HDR brachytherapy has since been extensively reported on by investigators in Europe, with control rates at 1 year on the order of 95% for single fraction treatments with peripheral doses of 25 Gy, and limited toxicity (106–111). In studies where patients had centrally located tumors adjacent to the liver hilum and bile duct bifurcation, multiple fraction regimens have been used, with up to five fractions in once or twice daily treatments (112,111); bile duct stenosis and post-hepatic cholestasis can result from treatment to this area (113). Single or multiple catheters can be placed under CT guidance and may be assisted with ultrasound techniques (114). For large tumors, interstitial brachytherapy has also been safely combined with transarterial chemoembolization to facilitate effective treatment (115).

Radioembolization may be limited by vascular access, shunting, functional liver reserve, and possibly by prior radiation (116–118,36,119,120). For liver brachytherapy, it is possible that patients could have lesions that are too large or advanced to treat effectively, although primary lesions as large as 12 cm (108,121) and metastatic lesions as large as 13.5 cm (109) in diameter have been successfully implanted in prospective studies. Patients with multiple lesions (five or more) may be technically too difficult to implant for interstitial brachytherapy. In these cases, lobar or whole liver radioembolization could be the preferred treatment. Patients with refractory coagulopathies would also be difficult to treat with percutaneous interstitial brachytherapy or TARE techniques, and noninvasive treatments such as stereotactic body radiation therapy may be the preferred treatment modality.

In terms of anatomic considerations, certain areas of the liver are of greater concern for effective and safe treatment with interstitial brachytherapy. Lesions at the periphery of the liver in close contact with viscera may not be optimal for large single-fraction interstitial brachytherapy treatments, and central liver lesions may also be associated with greater risks of bile duct stenosis with interstitial brachytherapy approaches. Lesions located high in the liver dome may be difficult to treat with interstitial approaches due to surrounding pleura and lung tissue; pleural penetration carries the risk of pneumothorax, which could be devastating in a cirrhotic patient, although this is less likely with the smaller needles used for interstitial brachytherapy than those used in other interventional radiology approaches. These patients may also derive more benefit from an SBRT or radioembolization approach.

Role of ^{90}Y TARE in surgical patients

Patients with metastatic colorectal cancer can only be cured with the use of multiple modalities: chemotherapy and surgery are the mainstay of treatment, with the use of liver directed therapy and radiation therapy in circumstances where these modalities augment and potentiate other therapies. The goal of this section is to outline the role of ^{90}Y TARE, in those patients that have metastatic colorectal cancer (mCRC) to the liver and for those that have primary hepatocellular carcinoma (HCC). Surgery after TARE can be performed safely, provided appropriate patient selection. Preservation of hepatic reserve, and anatomically clear margins of resection determine clinical outcome and risk of complication (122).

Surgical considerations for augmenting resectability

Surgeons have previously focused on the liver segments that are resected in planning their surgery. In fact, in recent years, the focus has changed to looking at the liver that is left behind after surgery. This is referred to as the Functional Liver Remnant (FLR) (123). As would be logical,

Please cite this article as: N.K. Sharma *et al.*, The American Brachytherapy Society consensus statement for permanent implant brachytherapy using Yttrium-90 microsphere radioembolization for liver tumors, Brachytherapy, https://doi.org/10.1016/j.brachy.2022.04.004

adequate FLR is impacted by degree of liver disease: the FLR can be as low as 25% in the case of a normal liver but must be 40% or greater in those with significant liver disease (124). Cross sectional imaging, either using MRI with a hepatocellular contrast agent or SPECT/CT with ^{99m}Tc-sulfur colloid or ^{99m}Tc-IDA agents, can be used by the HPB surgeon to evaluate the functional liver. As such, the HPB surgeon may focus on segment 2 and 3 of the left liver to examine carefully if this is free of disease. If this is the case, surgical resection of the right liver, leaving the left liver (segments 2,3,4, and 1) will be possible. Alternatively, if segment 4 has disease, an extended right liver resection (some call this trisection) is possible leaving just segments 2 and 3 (the left lateral section of the liver). This is a major liver resection, and this is the case where an augmentation with ^{90}Y TARE might be helpful. Alternatively, it would be appropriate to consider ^{90}Y TARE in those cases where the left liver volume is low, and the right lobe could then be treated with ^{90}Y TARE.

The goal of ^{90}Y TARE in this "radiation lobectomy" intent, would be to treat the sites of tumor (i.e., the segments of liver with tumor) and spare the FLR. Dosing and specifics of the treatment process have been discussed previously in this document. The intent here is to achieve ipsilateral atrophy and contralateral hypertrophy. It should be noted that this takes longer than when a portal vein embolization (PVE) is used for this intent: 6–8 weeks suffice with PVE (even less if hepatic vein occlusion is added), whereas 12 weeks is the minimum in cases of radiation lobectomy (125).

The treating team may consider keeping the patient off chemotherapy during the time after ^{90}Y lobectomy, if there is no active disease in lungs or other extrahepatic sites. The reasoning is that the liver metastases are being treated with ^{90}Y during the period that we are waiting for hypertrophy to develop. This will help minimize liver injury related to chemotherapy (outlined in section VI). The patient may then undergo a right or extended right liver resection.

Role of ^{90}Y TARE in augmenting margins

The margins of surgical resection have been shown to correlate with outcome in those patients that undergo surgical resection (122). Specifically, the available data suggest that the distance of margin correlates specifically with survival. The challenge is when a patient is a candidate for resection but has a minimal margin available for a major hepatic resection. Usually, this occurs when there is tumor close to a critical structure like the left hepatic vein in the case of an extended right liver resection. ^{90}Y TARE can be used in these cases to provide a radiation augmentation of the margin by effectively sterilizing the outer borders of the tumor. This concept has been used in pancreas cancer where preoperative chemotherapy or chemoradiotherapy may be used to achieve a similar result (126). This use of ^{90}Y TARE is not widely published but is an additional clinical scenario where it may be useful.

Role of ^{90}Y TARE to treat small lesions

Some patients have diffuse disease that will not allow for surgical resection of disease based on pretreatment volume of disease. These cases are like those eligible for the SIRFLOX study and it is common practice to invoke ^{90}Y TARE early in these patients (127). As noted in SIRFLOX, control of hepatic disease from colorectal metastases was excellent with ^{90}Y TARE and chemotherapy combined. As such, it is more common to use ^{90}Y TARE in those patients that have the greatest burden of disease in the liver. However, it is recommended to be especially cautious with those that have bulky nodal metastases as this may indicate aggressive biology.

It has been observed that some patients can have PET and MRI resolution of small lesions with the use of ^{90}Y TARE and chemotherapy. It is hypothesized that this is similar to the role of hepatic artery infusion (HAI), as published by the Memorial group (128). There is one retrospective and unmatched study that did not demonstrate an equivalence with HAI and ^{90}Y TARE (129). However, the patients were poorly matched with the ^{90}Y TARE patients having more extensive disease and poorer performance status.

In the circumstance that there are only a few PET or MRI visible lesions after a significant period of testing the tumor biology after^{90}Y TARE with chemotherapy, it is common practice to consider resection or ablation for these residual lesions. With this approach, in highly selected patients, there has been anecdotal long-term survival observed in patients treated by several authors of this document.

Hepatocellular carcinoma (HCC)

The role of ^{90}Y TARE in patients with HCC is in part dependent on whether they have cirrhosis or not. In those that do not have cirrhosis, the aim is to get the patient to some resection or aggressive ablation. In these cases, the algorithm and reasoning are much as outlined above for metastatic colorectal cancer (mCRC). The role of ^{90}Y TARE is especially valuable in testing the liver in those that are not cirrhotic but might have some fibrosis. In these cases, it may be possible to "stage the hit" to the liver by using ^{90}Y TARE and assessing how the liver tolerates this. If there is decompensation, proceeding to resection is not advised (130).

In those with cirrhosis, the role of ^{90}Y TARE is often to control disease and bridge the patient to transplantation. The whole liver is a fertile ground for further tumor growth and therefore liver replacement is really the preferred approach. Even in those with cirrhosis, as long as parameters for treatment eligibility (e.g., bilirubin $\leq$2, Childs-Pugh $\leq$B7, as described in other sections) are met, ^{90}Y TARE is well tolerated and effective (131).

Technical considerations in liver resection after ^{90}Y TARE

Traditionally there was some trepidation in the surgical community about the potential complications after liver re-

Please cite this article as: N.K. Sharma *et al.*, The American Brachytherapy Society consensus statement for permanent implant brachytherapy using Yttrium-90 microsphere radioembolization for liver tumors, Brachytherapy, https://doi.org/10.1016/j.brachy.2022.04.004

section in those patients that had received ^{90}Y. In fact, liver resection is safe after ^{90}Y TARE (132,133). In the authors' experience, ^{90}Y TARE can cause some adhesions especially to the vena cava and the diaphragm that can make the dissection somewhat harder. The liver that has been treated will look firmer and even somewhat fatty, making mobilization harder. However, this is all surmountable and ^{90}Y TARE is being used aggressively to augment and increase the population that are offered liver resection with curative intent.

Role of ^{90}Y TARE in patients considering proton therapy

Most of the proton beam's energy is deposited at a specific depth and within a narrow range known as the Bragg peak (134). As such, proton beam therapy (PBT) can deliver high tumor dose whereas sparing much of the uninvolved normal liver from any dose. PBT has a unique advantage over x-ray therapy (e.g., SBRT), which delivers a lower dose to potentially large volumes of the liver. The reduction in liver dose achieved with PBT is clinically meaningful for many liver cancer patients, especially those with cirrhosis, because of the association between even very low liver dose with the probability of radiation induced liver disease (RILD) (135–137).

A significant body of evidence has been accrued since the 1990s supporting PBT, typically delivered with ablative dose, as an appropriate treatment for liver cancer (138–143). In fact, PBT is endorsed by the National Comprehensive Cancer Network (NCCN) guidelines for some patients with HCC. Moreover, HCC is one of the few indications that receives the highest level of endorsement by the American Society for Radiation Oncology (ASTRO) in its Model Policy for Proton Beam Therapy (144,139,145,142). PBT for liver cancer other than HCC is increasingly being explored; mounting data suggesting that ablative PBT may improve LC and even OS compared to systemic therapy alone for selected patients with unresectable cholangiocarcinoma (139) or liver metastasis (146).

A spectrum of disease ranging from small solitary lesions to large and multifocal lesions may be appropriately treated with either PBT or ^{90}Y TARE because each modality can completely spare much of the normal liver whereas delivering high dose to tumor. There are no published comparisons of clinical outcomes between PBT and ^{90}Y TARE, however. Outcomes after ablative PBT for patients with larger tumors are noteworthy; 2- or 3-year LC exceeding 80–90% and less than 5% grade 3 or higher toxicity have been consistently reported for HCC patients with at least 5 cm median tumor size (147,144,148). Investigators from the University of Tsukuba reported outcomes of 22 patients with median 11 cm HCC (range 10–14) treated with PBT to a median 72.6 GyE in 22 fractions (biologically effective dose (BED_{10}): 96.6 Gy); 2-year local control for these sizeable tumors was 87% and no patient experienced grade 3 or higher toxicity (149). A separate study from the same group reported that 9 HCC patients with median 15 cm tumor (range 11–20) achieved 100% LC at median follow up of 13.7 months (150). A study from MD Anderson Cancer Center evaluated ablative salvage PBT for bilateral colorectal metastases not appropriate for second stage hepatectomy (151). Right hemi liver PBT was delivered to 5 patients with various ablative fractionation schedules with all achieving local control except for one who was prescribed the lowest dose; despite the large volume irradiated all patients were reported to have tolerated PBT well.

The distribution of tumor within the liver and volume of normal liver are important considerations for clinical decision making. Although the goal of having at least 700–800 cc of uninvolved liver has been established from the SBRT literature it remains unclear whether this is appropriate for PBT and ^{90}Y TARE (152,153). Compared to SBRT, PBT or ^{90}Y TARE may be more appropriate for some patients with multifocal liver cancer confined to one lobe or even limited disease in both lobes provided that sufficient normal liver sparing can be achieved. However, ^{90}Y TARE should typically be preferred over both SBRT and PBT for extensive multifocal bilobar disease because of its superior ability to minimize high and low-dose exposure to uninvolved liver.

There are important treatment delivery considerations for both liver PBT and ^{90}Y TARE. The liver is a moving target, which can perturb a proton beam, although there are effective motion management strategies and planning techniques that can ensure robust dose delivery and result in excellent long-term clinical outcomes (154–156). The exact range of a proton beam is uncertain and therefore a range uncertainty margin is added to ensure that the proton beam does not terminate until it traverses the target (157). High dose PBT conformality may therefore be sacrificed to improve precision. A notable limitation of ^{90}Y TARE is that dose metrics including high dose conformality are not known because routine dosimetric analysis is not incorporated into clinical practice. Emerging data show that incomplete tumor coverage and/or high liver doses from ^{90}Y TARE are associated with suboptimal efficacy and safety outcomes (72,75). A retrospective study by Allimant *et al.* using post-treatment PET/CT dosimetry demonstrated that 40% of HCC patients treated with resin ^{90}Y TARE microspheres had incomplete tumor targeting by the intended dose and that both median PFS and OS were inferior to patients with complete tumor targeting (both $p < 0.001$) (72). PBT may be a viable strategy to augment dose to tumor that was incompletely treated by ^{90}Y TARE whereas maintaining excellent normal liver sparing.

Combination with systemic agents

There is much interest in combining the use of ^{90}Y TARE with systemic agents (21,131,24). The major research focus has been on concurrent use, where there is

Please cite this article as: N.K. Sharma *et al.*, The American Brachytherapy Society consensus statement for permanent implant brachytherapy using Yttrium-90 microsphere radioembolization for liver tumors, Brachytherapy, https://doi.org/10.1016/j.brachy.2022.04.004

potential synergy between the radiation and systemic therapy, with several cytotoxic agents known to have radiation sensitizing properties. Activity of the systemic therapy outside the liver can also be beneficial in the many patients with metastatic disease that are otherwise good candidates for ^{90}Y TARE but also have low bulk extra-hepatic disease. Prospective randomized studies have now been completed in patients with metastatic colorectal cancer and hepatocellular cancer. Looking forward, the combination of ^{90}Y TARE with immune base therapy is a promising strategy, with several trials now exploring this combination.

Combining ^{90}Y TARE with chemotherapy to treat metastatic colorectal cancer (mCRC)

The largest bulk of research in combining ^{90}Y TARE with chemotherapy has been in patients with metastatic colorectal cancer (mCRC), a common tumor type that frequently metastasizes to the liver, often as the only site of metastatic disease. Initial studies in colorectal cancer combined ^{90}Y TARE with a fluoropyrimidine in an era where single agent therapy was the standard of care, with the known radiation sensitizing properties of fluoropyrimidines (158) adding to the attraction of this approach. The safety and efficacy of this combination was demonstrated in two small randomized studies (159,160), the second of which demonstrated an overall survival benefit. More recently, in patients with chemorefractory disease, adding SIRT microspheres to infusional 5FU was shown to prolong control of colorectal liver metastases (161). A single arm second line study in colorectal cancer, combining ^{90}Y TARE with a modified dose of irinotecan, also demonstrated safety and promising activity (162).

With the advent of combination chemotherapy as a standard of care in the first line setting, multiple studies were initiated to explore the safety and efficacy of ^{90}Y TARE in combination with oxaliplatin, this being part of the most frequently used doublet chemotherapy and oxaliplatin having known radiation sensitizing properties (25). As biologic therapy was soon thereafter integrated into standard of care practice for patients with metastatic treatment early, an early protocol amendment allowed clinicians the option of adding bevacizumab from cycle 4. A preplanned combined analysis of the three independent studies, all with similar eligibility criteria and treatment protocols, ultimately failed to show an impact on overall survival (25). The addition of ^{90}Y TARE did however significantly increase the liver response rate and delayed progression of metastatic disease in the liver. An independent blind review of liver images collected as part of the SIRFLOX study did demonstrate that more patients in the ^{90}Y TARE arm had technically resectable disease at the time of maximal treatment response (133). A retrospective analysis of the impact of primary tumor side, data that was collected prospectively in the SIRFLOX and FOXFIRE Global studies, demonstrated progression free and overall survival gains in the subset of patients with a right-sided primary (127). As this patient subset has a relatively poor prognosis and limited treatment options, due to limited benefit from agents targeting the epidermal growth factor receptor pathway, further studies enrolling only patients with a right-sided primary are justified. The combination of ^{90}Y TARE with regorafenib or with oral fluorothymidine agent, TAS102, agents that are now standard of care treatments for patients that have failed chemotherapy, is now being explored in clinical trials.

Combining ^{90}Y TARE with systemic therapy to treat hepatocellular cancer (HCC)

Sorafenib, an oral multi-kinase inhibitor, was shown to improve overall survival for patients with intermediate or advanced hepatocellular carcinoma (HCC) in two randomized placebo-controlled trials (163). This data stimulated enthusiasm for head-to-head studies to compare ^{90}Y TARE with sorafenib in patients with the Barcelona clinic liver cancer (BCLC) stage B or C HCC who had a ECOG performance status of 0–2 and good liver function (Child-Pugh A or B). The results of these trials were recently reviewed, along with four retrospective studies (163). Although ^{90}Y TARE was found to produce a higher response rate, the disease control rate and overall survival was similar to sorafenib. An analysis of grade 3 or 4 adverse events suggested that ^{90}Y TARE was better tolerated than sorafenib. The one-off treatment associated with ^{90}Y TARE may also be attractive to patients compared to the continuous dosing required with sorafenib, likely resulting in low grade adverse events whereas treatment is ongoing.

^{90Y} TARE plus systemic therapy in other tumor types

The safety and efficacy of ^{90}Y TARE has been explored in many other tumor types that metastasize to the liver, typically in patients with liver only or liver dominant disease that have failed standard therapy. To date varying degrees of activity have been reported along with the expected rates of adverse events but no randomized trials have been completed. In a recent review of the safety of combining systemic therapy with ^{90}Y TARE (164) the authors concluded that ^{90}Y TARE could be safely integrated into the standard of care for most cancer types, with caution advised with the use of VEGF inhibitors and gemcitabine. With these two agents sequential use is advisable, with the addition of bevacizumab 6 weeks post ^{90}Y TARE for patients with metastatic colorectal cancer (25) and gemcitabine 8 weeks post ^{90}Y TARE in patients with metastatic pancreas cancer (17) shown to be safe. In the pancreatic cancer study, as in many other studies across a broad range of metastatic tumor types, encouraging responses were seen in the liver but extra-hepatic progression limited any potential impact on overall survival.

^{90Y} TARE plus immunotherapy

The use of immune-based treatment has revolutionized the treatment and outcome for many solid tumor types.

Please cite this article as: N.K. Sharma *et al.*, The American Brachytherapy Society consensus statement for permanent implant brachytherapy using Yttrium-90 microsphere radioembolization for liver tumors, Brachytherapy, https://doi.org/10.1016/j.brachy.2022.04.004

Radiation therapy has potent immunomodulatory effects (165), with the potential for promotion of tumor specific immunity leading to disease response beyond the area targeted with radiation therapy (the abscopal effect). The potential of combining ^{90}Y TARE with immunotherapy is now being actively explored, motivated by the potential of SIRT to enhance response to immunotherapy within the liver and at more distant sites, across multiple tumor types. No outcome data from the current combination studies in colorectal cancer, hepatocellular cancer and ocular melanoma is yet available.

Summary

90Y TARE is a safe and effective treatment for management of patients with primary malignancies of the liver and metastatic disease in the liver.

90Y TARE should be tailored specifically to each patient's disease burden, treatment intent, and integrated appropriately into their continuum of cancer care.

Multidisciplinary discussion is essential to appropriately select patients for ^{90}Y TARE. Some of the clinical considerations may include:

Extend of disease: Liver dominant versus extra-hepatic tumor load

Treatment Intent: Palliation versus curative versus neoadjuvant

Prior loco-regional therapies (e.g., TACE, ablation, etc.)

Concurrent treatments such as chemotherapy or immunotherapy

There are multiple methodologies available for dosimetry calculations (single-compartment, partition, or voxel dosimetry models) and planned treatment doses depending on device used and treatment intent. Additional considerations may include:

Prior chemotherapy regiments

Prior radiation therapy regiments (e.g., ^{90}Y TARE, SBRT, etc.)

Underlying liver function and clinical laboratory values (e.g., bilirubin, albumin, etc.)

Use of advanced 3D imaging is strongly encouraged for both treatment planning and treatment verification:

^{99m}Tc-MAA SPECT/CT for assessment on intra and extra-hepatic MAA distribution and dosimetry treatment planning

CBCT to ensure complete tumor coverage during 90Y TARE

90Y SPECT/CT or PET/CT for verification of treatment delivery

Consistency in catheter location between planning MAA and treatment 90Y to improve concordance in biodistribution (except for radiation segmentectomy)

Use of appropriate follow-up imaging times (3 ± 1 months and 6 ± 1 months) and use of appropriate disease-specific response metrics (e.g., mRECIST or EASL for HCC, RECIST for mCRC). For instance, in most cases, one month may be too short to appreciate response status after ^{90}Y TARE.

Conclusions

^{90}Y TARE using commercially available glass or resin microspheres is an excellent brachytherapy modality for primary hepatic malignancies or metastatic disease that has spread from other sites to the liver. It is well-tolerated and by virtue of the beta emission properties of ^{90}Y delivered preferentially utilizing tumor vasculature, can deliver high (tumoricidal) doses whereas minimizing normal liver radiation exposure. ^{90}Y TARE can be used to treat liver tumors either as monotherapy, in conjunction with other local/systemic modalities or as neodjuvant/adjuvant treatment. A true multidisciplinary evaluation of each patients' eligibility for ^{90}Y TARE, their other treatment options and the ideal integration of this modality into the continuum of their cancer care is imperative for optimal patient selection. Accurate pre- and post-treatment dosimetry with appropriate use of available imaging and technology are essential to improving patient outcomes. An extensive breadth of multidisciplinary discussion and a practical, focused approach to answering current questions about patient selection and program implementation are features addressed in this ABS consensus statement.

Conflicts of Interest

Dr. Sharma received honoraria, research grant, and is a consultant for SIRTEX Medical Inc. Dr. Kappadath received honoraria and research funding from Boston Scientific, SIRTEX Medical, and ABK Biomedical. Dr. Choung received honoraria from SIRTEX Medical Inc. Dr Jabbour is a consultant for Merck & Co Inc; Syntactx, IMX Medical; and has grant funding from the NIH and Merck & Co, Inc. Dr Jeyarajah is a consultant for Angiodynamics, SIRTEX Medical Inc., Ethicon. Dr. Liu is a consultant for SIRTEX Medical Inc, Eisai Pharmaceuticals, and a speaker for Astra Zeneca and Eisa Pharmaceuticals. Dr. Meyer has a research grant and honorarium from Varian Medical Systems. Dr. Mikell has a research grant funding from Varian. Dr. Patel is a consultant to SIRTEX Medical and Medtronic Inc. and a speaker for Boston Scientific. Drs. Folkert, Kennedey, Gibbs, Yang, and Mourtada report no conflict of interest.

References

[1] Lee EW, Thakor AS, Tafti BA, Liu DM. Y90 selective internal radiation therapy. *Surg Oncol Clin N Am* 2015;24:167–185.

[2] Liu DM, Salem R, Bui JT, *et al.* Angiographic considerations in patients undergoing liver-directed therapy. *J Vasc Interv Radiol* Jul 2005;16:911–935.

Please cite this article as: N.K. Sharma *et al.*, The American Brachytherapy Society consensus statement for permanent implant brachytherapy using Yttrium-90 microsphere radioembolization for liver tumors, Brachytherapy, https://doi.org/10.1016/j.brachy.2022.04.004

[3] Lewandowski RJ, Sato KT, Atassi B, *et al.* Radioembolization with 90Y microspheres: angiographic and technical considerations. *Cardiovasc Intervent Radiol* Jul-Aug 2007;30(4):571–592.
[4] Berger MJ, Coursey JS, Zucker MA, Chang J. ESTAR, PSTAR, and ASTAR: computer programs for calculating stopping-power and range tables for electrons, protons, and helium ions, 2005.
[5] Erbe EM, Day DE. Chemical durability of Y2O3-Al2O3-SiO2 glasses for the in vivo delivery of beta radiation. *J Biomed Mater Res* Oct 1993;27:1301–1308.
[6] Biocompatibles; Therasphere (TM). Package Insert. Biocompatibles UK Ltd, Chapman House Farnham Business Park Weydon Lane FARNHAM, GU9 8QL United Kingdom, 2014.
[7] Day D.E., Ehrhardt G.J. Microspheres for radiation therapy. 1994.
[8] Sirtex SIR-Sphere (TM). package insert. *Sirtex Medical Inc* 2011.
[9] Gray B.N. Method of treating cancer. 2014.
[10] SIR-Sphere (TM). package insert. *Sirtex Medical Inc* 2011.
[11] Ahmadzadehfar H, Meyer C, Pieper CC, *et al.* Evaluation of the delivered activity of yttrium-90 resin microspheres using sterile water and 5% glucose during administration. *EJNMMI Res* 2015;5:54 2015/10/13.
[12] Koran ME, Stewart S, Baker JC, *et al.* Five percent dextrose maximizes dose delivery of Yttrium-90 resin microspheres and reduces rates of premature stasis compared to sterile water. *Biomed Rep* 2016;5:745–748 2016/12.
[13] Paprottka KJ, Lehner S, Fendler WP, *et al.* Reduced periprocedural analgesia after replacement of water for injection with glucose 5% solution as the infusion medium for 90Y-resin microspheres. *J Nucl Med* 2016;57:1679–1684 2016/11/01.
[14] Helling TS, Martin M. Cause of death from liver metastases in colorectal cancer. *Ann Surg Oncol* 2014;21:501–506.
[15] Abdalla EK, Vauthey JN, Ellis LM, *et al.* Recurrence and outcomes following hepatic resection, radiofrequency ablation, and combined resection/ablation for colorectal liver metastases. *Ann Surg* 2004;239:818–825 discussion 25-7.
[16] Ruers T, Van Coevorden F, Punt CJ, *et al.* Local Treatment of unresectable colorectal liver metastases: results of a randomized phase II trial. *J Natl Cancer Inst* 2017;109:1–10.
[17] Gibbs P, Do C, Lipton L, *et al.* Phase II trial of selective internal radiation therapy and systemic chemotherapy for liver-predominant metastases from pancreatic adenocarcinoma. *BMC Cancer* 2015;15:802.
[18] Tempero MA, Arnoletti JP, Behrman SW, *et al.* Pancreatic adenocarcinoma, version 2.2012: featured updates to the NCCN guidelines. *J Natl Compr Canc Netw* 2012;10:703–713.
[19] Seufferlein T, Porzner M, Becker T, *et al.* [S3-guideline exocrine pancreatic cancer]. *Z Gastroenterol* 2013;51:1395–1440.
[20] Sangha BS, Nimeiri H, Hickey R, *et al.* Radioembolization as a treatment strategy for metastatic colorectal cancer to the liver: what can we learn from the SIRFLOX trial? *Curr Treat Options Oncol* 2016;17:26 06.
[21] van Hazel GA, Heinemann V, Sharma NK, *et al.* SIRFLOX: randomized phase III trial comparing first-line mFOLFOX6 (Plus or Minus Bevacizumab) versus mFOLFOX6 (Plus or Minus Bevacizumab) plus selective internal radiation therapy in patients with metastatic colorectal cancer. *J Clin Oncol* 2016;34:1723–1731 05.
[22] Kennedy A, Cohn M, Coldwell DM, *et al.* Updated survival outcomes and analysis of long-term survivors from the MORE study on safety and efficacy of radioembolization in patients with unresectable colorectal cancer liver metastases. *J Gastrointest Oncol* 2017;8:614–624.
[23] Salem R, Gabr A, Riaz A, *et al.* Institutional decision to adopt Y90 as primary treatment for hepatocellular carcinoma informed by a 1,000-patient 15-year experience. *Hepatology* 2018;68:1429–1440.
[24] Teyateeti A, Mahvash A, Long JP, *et al.* Survival outcomes for Yttrium-90 transarterial radioembolization with and without sorafenib for unresectable hepatocellular carcinoma patients. *J Hepatocell Carcinoma* 2020;7:117–131.
[25] Wasan HS, Gibbs P, Sharma NK, *et al.* First-line selective internal radiotherapy plus chemotherapy versus chemotherapy alone in patients with liver metastases from colorectal cancer (FOXFIRE, SIRFLOX, and FOXFIRE-Global): a combined analysis of three multicentre, randomised, phase 3 trials. *Lancet Oncol* 2017;18:1159–1171 09.
[26] Cucchetti A, Sposito C, Pinna AD, *et al.* Competing risk analysis on outcome after hepatic resection of hepatocellular carcinoma in cirrhotic patients. *World J Gastroenterol* 2017;23:1469–1476.
[27] Malhotra A, Liu DM, Talenfeld AD. Radiation segmentectomy and radiation lobectomy: a practical review of techniques. *Tech Vasc Interv Radiol* 2019;22:49–57.
[28] Padia SA, Lewandowski RJ, Johnson GE, *et al.* Radioembolization of hepatic malignancies: background, quality improvement guidelines, and future directions. *J Vasc Interv Radiol* 2017;28:1–15.
[29] Bishay VL, Biederman DM, Ward TJ, *et al.* Transradial approach for hepatic radioembolization: initial results and technique. *AJR Am J Roentgenol* 2016;207:1112–1121.
[30] Ng E, Chung J, Klass D, *et al.* Optimized computed tomographic angiography vessel evaluation protocol (OCTAVE) prior to trans-arterial radioembolization. *Intervent Oncol* 2016;360:E183–EE93 4.
[31] Hamoui N, Minocha J, Memon K, *et al.* Prophylactic embolization of the gastroduodenal and right gastric arteries is not routinely necessary before radioembolization with glass microspheres. *J Vasc Interv Radiol* 2013;24:1743–1745.
[32] Schelhorn J, Theysohn J, Ertle J, *et al.* Selective internal radiation therapy of hepatic tumours: is coiling of the gastroduodenal artery always beneficial? *Clin Radiol* 2014;69:e216–e222.
[33] Borggreve AS, Landman A, Vissers CMJ, *et al.* Radioembolization: is prophylactic embolization of hepaticoenteric arteries necessary? A systematic review. *Cardiovasc Intervent Radiol* 2016;39:696–704.
[34] Fischman A, Patel R, Kim E. COSY trial: a prospective, randomized study of coilng vs surefire infusion system in Y90. *J Vasc and Interventional Radiol* 2014;25:S107–SS08.
[35] Bhalani SM, Lewandowski RJ. Radioembolization complicated by nontarget embolization to the falciform artery. *Semin Intervent Radiol* 2011;28:234–239.
[36] Wang DS, Louie JD, Kothary N, *et al.* Prophylactic topically applied ice to prevent cutaneous complications of nontarget chemoembolization and radioembolization. *J Vasc Interv Radiol* 2013;24:596–600.
[37] Louie JD, Kothary N, Kuo WT, *et al.* Incorporating cone-beam CT into the treatment planning for yttrium-90 radioembolization. *J Vasc Interv Radiol* 2009;20:606–613.
[38] Ahmadzadehfar H, Sabet A, Biermann K, *et al.* The significance of 99mTc-MAA SPECT/CT liver perfusion imaging in treatment planning for 90Y-microsphere selective internal radiation treatment. *J Nucl Med* 2010;51:1206–1212.
[39] Haggerty JE, Vaidya S, Kooy T, *et al.* Identification of the falciform artery on nuclear medicine imaging with successful coil embolization for planned Y-90 therapy. *Clin Nucl Med* 2012;37:105–107.
[40] Haste P, Tann M, Persohn S, *et al.* Correlation of Technetium-99m macroaggregated albumin and Yttrium-90 glass microsphere biodistribution in hepatocellular carcinoma: a retrospective review of pretreatment single photon emission CT and posttreatment positron emission tomography/CT. *J Vasc Interv Radiol* 2017;28:722–730 e1.
[41] Yu N, Srinivas SM, DiFilippo FP, *et al.* Lung dose calculation with SPECT/CT for 90Yittrium radioembolization of liver cancer. *Int J Radiation Oncol*Biol*Physics* 2013;85:834–839 2013/03/01.
[42] Elschot M, Nijsen JFW, Lam MGEH, *et al.* 99mTc-MAA overestimates the absorbed dose to the lungs in radioembolization: a quantitative evaluation in patients treated with 166Ho-microspheres. *Eur J Nucl Med Mol Imaging* 2014;41:1965–1975 2014/05/13.

Please cite this article as: N.K. Sharma *et al.*, The American Brachytherapy Society consensus statement for permanent implant brachytherapy using Yttrium-90 microsphere radioembolization for liver tumors, Brachytherapy, https://doi.org/10.1016/j.brachy.2022.04.004

[43] Kao YH, Magsombol BM, Toh Y, *et al.* Personalized predictive lung dosimetry by technetium-99m macroaggregated albumin SPECT/CT for yttrium-90 radioembolization. *EJNMMI Res* 2014;4:33 2014/06/29.
[44] Allred JD, Niedbala J, Mikell JK, *et al.* The value of 99mTc-MAA SPECT/CT for lung shunt estimation in 90Y radioembolization: a phantom and patient study. *EJNMMI Res* 2018;8:50 2018/06/15.
[45] Dittmann H, Kopp D, Kupferschlaeger J, *et al.* A prospective study of quantitative SPECT/CT for evaluation of lung shunt fraction before SIRT of liver tumors. *J Nucl Med* 2018;59:1366–1372 2018/09/01.
[46] Lopez B, Mahvash A, Lam M, Kappadath SC. Calculation of lung mean dose and quantification of error for (90) Y-microsphere radioembolization using (99m) Tc-MAA SPECT/CT and diagnostic chest CT. *Med Phys* 2019;46:3929–3940.
[47] Ho CL, Chen S, Cheung SK, *et al.* Radioembolization with 90Y glass microspheres for hepatocellular carcinoma: significance of pretreatment 11C-acetate and 18F-FDG PET/CT and posttreatment 90Y PET/CT in individualized dose prescription. *Eur J Nucl Med Mol Imaging* 2018;45:2110–2121 2018/11/01.
[48] Busse N, Erwin W, Pan T. Evaluation of a semiautomated lung mass calculation technique for internal dosimetry applications. *Med Phys* 2013;40:122503 2013/12/01.
[49] Bastiaannet R, Viergever MA, dHWAM Jong. Impact of respiratory motion and acquisition settings on SPECT liver dosimetry for radioembolization. *Med Phys* 2017;44:5270–5279 2017/10/01.
[50] Mikell JK, Mahvash A, Siman W. Comparing voxel-based absorbed dosimetry methods in tumors, liver, lung, and at the liver-lung interface for (90)Y microsphere selective internal radiation therapy. *EJNMMI Phys* Dec 2015;2:16.
[51] Kappadath SC, Lopez BP, Salem R, Lam MG. Lung shunt and lung dose calculation methods for radioembolization treatment planning. *Q J Nucl Med Mol Imaging* 2021;65:32–42.
[52] Kappadath SC, Lopez BP, Salem R, Lam MGEH. Reassessment of the lung dose limits for radioembolization. *Nucl Med Commun* 2021;42:1064–1075.
[53] Lam MG, Banerjee A, Goris ML, *et al.* Fusion dual-tracer SPECT-based hepatic dosimetry predicts outcome after radioembolization for a wide range of tumour cell types. *Eur J Nucl Med Mol Imaging* Jul 2015;42:1192–1201.
[54] Willowson KP, Schembri GP, Bernard EJ, Chan DL. Quantifying the effects of absorbed dose from radioembolisation on healthy liver function with [(99m)Tc]TcMebrofenin. *Eur J Nucl Med Mol Imaging* Apr 2020;47:838–848.
[55] Gulec SA, Sztejnberg ML, Siegel JA. Hepatic structural dosimetry in (90)Y microsphere treatment: a Monte Carlo modeling approach based on lobular microanatomy. *J Nucl Med* 2010;51:301–310.
[56] Liu D, Klass D, Westcott M, Kennedy AS. The limitations of theoretical dose modeling for yttrium-90 radioembolization. *J Vasc Interv Radiol* 2014;25:1146–1147.
[57] Henry E, Strugari M, Mawko G, *et al.* Post-administration dosimetry in yttrium-90 radioembolization through micro-CT imaging of radiopaque microspheres in a porcine renal model. *Phys Med Biol* 2021;66. doi:10.1088/1361-6560/abf38a.
[58] Westcott MA, Coldwell DM, Liu DM, Zikria JF. The development, commercialization, and clinical context of yttrium-90 radiolabeled resin and glass microspheres. *Adv Radiat Oncol* 2016;1:351–364.
[59] Liu D, Westcott M, Garcia-Monaco R, Abraham R. Down and dirty with Dosimetry A practical understanding and approach to radioembolization. *Endovascular Today* 2016:15.
[60] Lam MGEH, Louie JD, Abdelmaksoud MHK. Limitations of body surface area–based activity calculation for radioembolization of hepatic metastases in colorectal cancer. *J Vasc and Interventional Radiol* 2014;25:1085–1093 2014/07.
[61] Ho S, Lau WY, Leung TW, *et al.* Partition model for estimating radiation doses from yttrium-90 microspheres in treating hepatic tumours. *Eur J Nucl Med* 1996;23:947–952 1996/08.
[62] Bolch WE, Bouchet LG, Robertson JS. MIRD Pamphlet No. 17: the dosimetry of nonuniform activity distributions–radionuclide s values at the voxel level. *J Nucl Med* 1999;40:11S–136 1999/01/01.
[63] Dieudonne A, Hobbs RF, Bolch WE. Fine-resolution voxel s values for constructing absorbed dose distributions at variable voxel size. *J Nucl Med* 2010;51:1600–1607 2010/10/01.
[64] Amato E., Minutoli F., Pacilio M., *et al.* An analytical method for computing voxel S values for electrons and photons. Med Physics. 2012 2012/11/01;39:6808–17.
[65] Lanconelli N, Pacilio M, Lo Meo S. A free database of radionuclide voxel S values for the dosimetry of nonuniform activity distributions. *Phys Med Biol* 2012;57:517–533 2012/01/21.
[66] Sanchez-Garcia M, Gardin I, Lebtahi R, Dieudonné A. A new approach for dose calculation in targeted radionuclide therapy (TRT) based on collapsed cone superposition: validation with 90Y. *Phys Med Biol* 2014;59:4769 2014/09/07.
[67] Mikell J, Kappadath SC, Wareing T. Evaluation of a deterministic grid-based Boltzmann solver (GBBS) for voxel-level absorbed dose calculations in nuclear medicine. *Phys Med Biol* 2016;61:4564 2016.
[68] Prideaux AR, Song H, Hobbs RF. Three-dimensional radiobiologic dosimetry: application of radiobiologic modeling to patient-specific 3-dimensional imaging-based internal Dosimetry. *J Nucl Med* 2007;48:1008–1016 2007/06/01.
[69] Pasciak AS, Erwin WD. Effect of voxel size and computation method on Tc-99m MAA SPECT/CT-based dose estimation for Y-90 microsphere therapy. *IEEE Trans Med Imaging* 2009;28:1754–1758 2009/11.
[70] Dieudonné A, Hobbs RF, Lebtahi R. Study of the impact of tissue density heterogeneities on 3-dimensional abdominal dosimetry: comparison between dose kernel convolution and direct Monte Carlo methods. *J Nucl Med* 2013;54:236–243 2013/02/01.
[71] Mikell JK, Mahvash A, Siman W. Selective internal radiation therapy with yttrium-90 glass microspheres: biases and uncertainties in absorbed dose calculations between clinical dosimetry models. *Int J Radiation Oncol*Biol*Physics* 2016;96:888–896 2016/11/15.
[72] Allimant C, Kafrouni M, Delicque J, *et al.* Tumor targeting and three-dimensional voxel-based dosimetry to predict tumor response, toxicity, and survival after Yttrium-90 resin microsphere radioembolization in hepatocellular carcinoma. *J Vasc and Interventional Radiol* 2018;29:1662–1670 2018/12/01e4..
[73] Siman W, Mawlawi OR, Mikell JK, Mourtada F. Effects of image noise, respiratory motion, and motion compensation on 3D activity quantification in count-limited PET images. *Phys Med Biol* 2017;62:448 2017.
[74] Siman W, Mawlawi OR, Mourtada F, Kappadath SC. Systematic and random errors of PET-based (90) Y 3D dose quantification. *Med Phys* 2020;47:2441–2449.
[75] Kappadath SC, Mikell J, Balagopal A. Hepatocellular carcinoma tumor dose response after (90)Y-radioembolization with glass microspheres using (90)Y-SPECT/CT-based voxel dosimetry. *Int J Radiat Oncol Biol Phys* 2018;102:451–461.
[76] Balagopal A, Kappadath SC. Characterization of 90Y-SPECT/CT self-calibration approaches on the quantification of voxel-level absorbed doses following 90Y-microsphere selective internal radiation therapy. *Med Phys* 2017;45:875–883.
[77] Lhommel R, vL Elmbt, Goffette P. Feasibility of 90Y TOF PET-based dosimetry in liver metastasis therapy using SIR-Spheres. *Eur J Nucl Med Mol Imaging* 2010;37:1654–1662 2010/08/01.
[78] Fourkal E, Veltchev I, Lin M. 3D inpatient dose reconstruction from the PET-CT imaging of 90Y microspheres for metastatic cancer to the liver: feasibility study. *Med Phys* 2013;40:081702.
[79] Carlier T., Willowson K.P., Fourkal E., *et al.* 90Y -PET imaging: exploring limitations and accuracy under conditions of low counts and high random fraction. Medical Physics. 2015 2015/07/01;42:4295–309.

Please cite this article as: N.K. Sharma *et al.*, The American Brachytherapy Society consensus statement for permanent implant brachytherapy using Yttrium-90 microsphere radioembolization for liver tumors, Brachytherapy, https://doi.org/10.1016/j.brachy.2022.04.004

[80] Willowson KP, Tapner M, Bailey DL. A multicentre comparison of quantitative 90Y PET/CT for dosimetric purposes after radioembolization with resin microspheres. *Eur J Nucl Med Mol Imaging* 2015;42:1202–1222 2015.
[81] D'Arienzo M, Chiaramida P, Chiacchiararelli L. 90Y PET-based dosimetry after selective internal radiotherapy treatments. *Nuclear Medicine Communications June 2012* 2012;33:633–640 2012.
[82] Siman W, Kappadath SC. Comparison of step-and-shoot and continuous-bed-motion PET modes of acquisition for limited-view organ scans. *J Nucl Med Technol* Dec 2017;45:290–296.
[83] Siman W, Mikell JK, Mawlawi OR. Dose volume histogram-based optimization of image reconstruction parameters for quantitative (90) Y-PET imaging. *Med Phys* 2019;46:229–237.
[84] Siman W, Mikell JK, Kappadath SC. Practical reconstruction protocol for quantitative 90Y bremsstrahlung SPECT/CT. *Med. Phys.* 2016:5093–5103. 2016/09/01.
[85] Rong X, Du Y, Ljungberg M. Development and evaluation of an improved quantitative [sup 90]Y bremsstrahlung SPECT method. *Med Phys* 2012;39:2346–2358 2012.
[86] Elschot M, Lam MGEH, vdMAAJ Bosch. Quantitative Monte Carlo–based 90Y SPECT reconstruction. *J Nucl Med* 2013:1557–1563. 2013/09/01.
[87] Dewaraja YK, Chun SY, Srinivasa RN. Improved quantitative 90Y bremsstrahlung SPECT/CT reconstruction with Monte Carlo scatter modeling. *Med Phys* 2017;12:6364–6376 2017/44.
[88] Lim H, Fessler JA, Wilderman SJ. Y-90 SPECT ML image reconstruction with a new model for tissue-dependent bremsstrahlung production using CT information: a proof-of-concept study. *Phys Med Biol* 2018;63:115001 2018.
[89] Ng SC, Lee VH, Law MW. Patient dosimetry for 90Y selective internal radiation treatment based on 90Y PET imaging. *J Appl Clin Med Phys* 2013;14:212–221.
[90] Martí-Climent JM, Prieto E, Elosúa C. PET optimization for improved assessment and accurate quantification of 90Y-microsphere biodistribution after radioembolization. *Med Phys* 2014;41:092503.
[91] Wright CL, Zhang J, Binzel K. 90Y Digital PET/CT imaging following radioembolization. *Clin Nucl Med* 2016;41:975–976.
[92] Knešaurek K, Tuli A, Kim E, *et al.* Comparison of PET/CT and PET/MR imaging and dosimetry of yttrium-90 (90Y) in patients with unresectable hepatic tumors who have received intra-arterial radioembolization therapy with 90Y microspheres. *EJNMMI Phys* 2018;5(1):23. doi:10.1186/s40658-018-0222-y.
[93] Eckerman K, Endo A. ICRP Publication 107. Nuclear decay data for dosimetric calculations. *Ann ICRP* 2008 2008;38:7–96.
[94] Zanzonico PB, Binkert BL, Goldsmith SJ. Bremsstrahlung radiation exposure from pure β-Ray emitters. *J Nucl Med* 1999;40:1024–1028 1999/06/01.
[95] Gulec SA, Siegel JA. Posttherapy radiation safety considerations in radiomicrosphere treatment with 90Y-microspheres. *J Nucl Med* 2007;48:2080–2086 2007/12/01.
[96] Dezarn WA, Cessna JT, DeWerd LA. Recommendations of the American Association of Physicists in Medicine on dosimetry, imaging, and quality assurance procedures for [sup 90]Y microsphere brachytherapy in the treatment of hepatic malignancies. *Med Phys* 2011;38:4824–4845 2011.
[97] Giammarile F, Bodei L, Chiesa C. EANM procedure guideline for the treatment of liver cancer and liver metastases with intra-arterial radioactive compounds. *Eur J Nucl Med Mol Imaging* 2011;38:1393–1406 2011/04/15.
[98] Erwin W.D. Radiation safety concerns associated with preparing the dosage, treating and releasing the patient, and managing radioactive waste. Handbook of Radioembolization 2016.
[99] Thomas MA, Mahvash A, Abdelsalam M. Planning dosimetry for (90) Y radioembolization with glass microspheres: evaluating the fidelity of (99m) Tc-MAA and partition model predictions. *Med Phys* 2020;47:5333–5342.
[100] Mahvash A, Chartier S, Turco M. A prospective, multicenter, open-label, clinical trial design to evaluate the safety and efficacy of 90Y resin microspheres for treatment of unresectable hepatocellular carcinoma (HCC): dOORwaY90. *HPB* 2021;23:S545–SS46.
[101] Salem R, Padia SA, Lam M. Clinical and dosimetric considerations for Y90: recommendations from an international multidisciplinary working group. *Eur J Nucl Med Mol Imaging* 2019;46:1695–1704.
[102] Levillain H, Bagni O, Deroose CM. International recommendations for personalised selective internal radiation therapy of primary and metastatic liver diseases with yttrium-90 resin microspheres. *Eur J Nucl Med Mol Imaging* 2021;48(5):1570–1584.
[103] Lam MG, Abdelmaksoud MH, Chang DT. Safety of 90Y radioembolization in patients who have undergone previous external beam radiation therapy. *Int J Radiat Oncol Biol Phys* 2013;87:323–329.
[104] Wang TH, Huang PI, Hu YW. Combined Yttrium-90 microsphere selective internal radiation therapy and external beam radiotherapy in patients with hepatocellular carcinoma: from clinical aspects to dosimetry. *PLoS ONE* 2018;13:e0190098.
[105] Dritschilo A, Grant EG, Harter KW. Interstitial radiation therapy for hepatic metastases: sonographic guidance for applicator placement. *AJR Am J Roentgenol* 1986;147:275–278.
[106] Ricke J, Wust P, Stohlmann A. CT-guided interstitial brachytherapy of liver malignancies alone or in combination with thermal ablation: phase I-II results of a novel technique. *Int J Radiat Oncol Biol Phys* 2004;58:1496–1505.
[107] Ricke J, Wust P, Wieners G. Liver malignancies: cT-guided interstitial brachytherapy in patients with unfavorable lesions for thermal ablation. *J Vasc Interv Radiol* 2004;15:1279–1286.
[108] Mohnike K, Wieners G, Schwartz F. Computed tomography-guided high-dose-rate brachytherapy in hepatocellular carcinoma: safety, efficacy, and effect on survival. *Int J Radiat Oncol Biol Phys* 2010;78:172–179.
[109] Ricke J, Mohnike K, Pech M. Local response and impact on survival after local ablation of liver metastases from colorectal carcinoma by computed tomography-guided high-dose-rate brachytherapy. *Int J Radiat Oncol Biol Phys* 2010;78:479–485.
[110] Collettini F, Singh A, Schnapauff D. Computed-tomography-guided high-dose-rate brachytherapy (CT-HDRBT) ablation of metastases adjacent to the liver hilum. *Eur J Radiol* 2013;82:e509–e514.
[111] Tselis N, Chatzikonstantinou G, Kolotas C. Computed tomography-guided interstitial high dose rate brachytherapy for centrally located liver tumours: a single institution study. *Eur Radiol* 2013;23:2264–2270.
[112] Tselis N, Chatzikonstantinou G, Kolotas C. Hypofractionated accelerated computed tomography-guided interstitial high-dose-rate brachytherapy for liver malignancies. *Brachytherapy* 2012;11:507–514.
[113] Powerski M, Penzlin S, Hass P. Biliary duct stenosis after image-guided high-dose-rate interstitial brachytherapy of central and hilar liver tumors: a systematic analysis of 102 cases. *Strahlenther Onkol* 2019;195:265–273.
[114] Damm R, El-Sanosy S, Omari J. Ultrasound-assisted catheter placement in CT-guided HDR brachytherapy for the local ablation of abdominal malignancies: initial experience. *Rofo* 2019;191:48–53.
[115] Collettini F, Jonczyk M, Meddeb A. Feasibility and safety of CT-guided high-dose-rate brachytherapy combined with transarterial chemoembolization using irinotecan-loaded microspheres for the treatment of large, unresectable colorectal liver metastases. *J Vasc Interv Radiol* Feb 2020;31:315–322.
[116] Rhim H, Goldberg SN, Dodd GD 3rd. Essential techniques for successful radio-frequency thermal ablation of malignant hepatic tumors. *Radiographics* 2001:S17–S35 Oct21 Spec Nodiscussion S36-9.
[117] Kuvshinoff BW, Ota DM. Radiofrequency ablation of liver tumors: influence of technique and tumor size. *Surgery* 2002;132:605–611 discussion 11-2.

Please cite this article as: N.K. Sharma *et al.*, The American Brachytherapy Society consensus statement for permanent implant brachytherapy using Yttrium-90 microsphere radioembolization for liver tumors, Brachytherapy, https://doi.org/10.1016/j.brachy.2022.04.004

[118] Pan CC, Kavanagh BD, Dawson LA. Radiation-associated liver injury. *Int J Radiat Oncol Biol Phys* 2010 Mar 1;76(3):S94–100 Suppl.
[119] Kennedy A. Radioembolization of hepatic tumors. *J Gastrointest Oncol* 2014;5:178–189.
[120] Kennedy AS. Radiation oncology approaches in liver malignancies. *Am Soc Clin Oncol Educ Book* 2014:e150–e155.
[121] Collettini F, Schnapauff D, Poellinger A. Hepatocellular carcinoma: computed-tomography-guided high-dose-rate brachytherapy (CT-H-DRBT) ablation of large (5-7cm) and very large (>7cm) tumours. *Eur Radiol* 2012;22:1101–1109.
[122] Pardo F, Sangro B, Lee RC, *et al.* The Post-SIR-Spheres Surgery Study (P4S): retrospective analysis of safety following hepatic resection or transplantation in patients previously treated with selective internal radiation therapy with yttrium-90 resin microspheres. *Annals of surgical oncology* 2017;24:2465–2473 9.
[123] Kishi Yoji, Vauthey Jean-Nicolas. Issues to be considered to address the future liver remnant prior to major hepatectomy. *Surgery Today* 2021;51:472–484 4.
[124] Madoff DC, David C, Abdalla Ek Fau, Vauthey Jean-Nicolas. Portal vein embolization in preparation for major hepatic resection: evolution of a new standard of care. *Journal of vascular and interventional radiology* 2005;16:779–790 6.
[125] Gabr A, Polineni P, Mouli SK, *et al.* Neoadjuvant radiation lobectomy as an alternative to portal vein embolization in hepatocellular carcinoma. *Seminars in nuclear medicine* 2019;49(3).
[126] Zhang E, Wang L, Shaikh T, *et al.* Neoadjuvant chemoradiation impacts the prognostic effect of surgical margin status in pancreatic adenocarcinoma. *Annals of surgical oncology* 2022;29:354–363 1.
[127] Gibbs P, Heinemann V, Sharma NK. Effect of primary tumor side on survival outcomes in untreated patients with metastatic colorectal cancer when selective internal radiation therapy is added to chemotherapy: combined analysis of two randomized controlled studies. *Clin Colorectal Cancer* 2018;12:e617–ee29.
[128] Sofocleous CT, Garcia AR, Pandit-Taskar N, *et al.* Phase I trial of selective internal radiation therapy for chemorefractory colorectal cancer liver metastases progressing after hepatic arterial pump and systemic chemotherapy. *Clinical Colorectal Cancer* 2014;13:27–36 1.
[129] Dhir M, Zenati MS, Jones HL, *et al.* Effectiveness of hepatic artery infusion (HAI) versus selective internal radiation therapy (Y90) for pretreated isolated unresectable colorectal liver metastases (IU-CR-CLM). *Annals of Surgical Oncology* 2018;25:550–557 2.
[130] Kulik LM, Atassi B, van Holsbeeck L. Yttrium-90 microspheres (TheraSphere) treatment of unresectable hepatocellular carcinoma: downstaging to resection, RFA and bridge to transplantation. *J Surg Oncol* 2006;94:572–586.
[131] Ricke J, Klumpen HJ, Amthauer H. Impact of combined selective internal radiation therapy and sorafenib on survival in advanced hepatocellular carcinoma. *J Hepatol* 2019;71:1164–1174.
[132] Henry LR, Hostetter RB, Ressler B. Liver resection for metastatic disease after y90 radioembolization: a case series with long-term follow-up. *Ann Surg Oncol* 2015;22:467–474.
[133] Garlipp B, Gibbs P, Van Hazel GA. Secondary technical resectability of colorectal cancer liver metastases after chemotherapy with or without selective internal radiotherapy in the randomized SIRFLOX trial. *Br J Surg* 2019;12:1837–1846.
[134] Engelsman M, Schwarz M, Dong L. Physics controversies in proton therapy. *Semin Radiat Oncol* 2013;23:88–96.
[135] Dawson LA, Normolle D, Balter JM. Ten Haken RK. Analysis of radiation-induced liver disease using the Lyman NTCP model. *Int J Radiat Oncol Biol Phys* 2002;53:810–821.
[136] Dawson LA, Ten Haken RK. Partial volume tolerance of the liver to radiation. *Semin Radiat Oncol* 2005;15:279–283.
[137] Mizumoto M, Okumura T, Hashimoto T. Evaluation of liver function after proton beam therapy for hepatocellular carcinoma. *Int J Radiat Oncol Biol Phys* 2012 Mar 1;82:e529–e535.
[138] Mizumoto M, Okumura T, Hashimoto T. Proton beam therapy for hepatocellular carcinoma: a comparison of three treatment protocols. *Int J Radiat Oncol Biol Phys* 2011;81:1039–1045.
[139] Makita C, Nakamura T, Takada A. Clinical outcomes and toxicity of proton beam therapy for advanced cholangiocarcinoma. *Radiat Oncol* 2014;9:26.
[140] Apisarnthanarax S, Bowen SR, Combs SE. Proton beam therapy and carbon ion radiotherapy for hepatocellular carcinoma. *Semin Radiat Oncol* 2018;28:309–320.
[141] Chadha AS, Gunther JR, Hsieh CE. Proton beam therapy outcomes for localized unresectable hepatocellular carcinoma. *Radiother Oncol* 2019;133:54–61.
[142] Chuong MD, Kaiser A, Khan F. Consensus report from the Miami liver proton therapy conference. *Front Oncol.* 2019;9:457.
[143] Sanford NN, Pursley J, Noe B. Protons versus photons for unresectable hepatocellular carcinoma: liver decompensation and overall survival. *Int J Radiat Oncol Biol Phys* 2019;105:64–72.
[144] Komatsu S, Fukumoto T, Demizu Y. Clinical results and risk factors of proton and carbon ion therapy for hepatocellular carcinoma. *Cancer* 2011;117:4890–4904.
[145] ASTRO. Model policy for proton beam therapy. 2018.
[146] Hong TS, Wo JY, Borger DR. Phase II study of proton-based stereotactic body radiation therapy for liver metastases: importance of tumor genotype. *JNCI: Journal of the National Cancer Institute* 2017;109 9djx031.
[147] Kawashima M, Furuse J, Nishio T. Phase II study of radiotherapy employing proton beam for hepatocellular carcinoma. *J Clin Oncol* 2005;23:1839–1846.
[148] Hong TS, Wo JY, Yeap BY. Multi-institutional phase II study of high-dose hypofractionated proton beam therapy in patients with localized, unresectable hepatocellular carcinoma and intrahepatic cholangiocarcinoma. *J Clin Oncol* 2016;34:460–468.
[149] Sugahara S, Oshiro Y, Nakayama H. Proton beam therapy for large hepatocellular carcinoma. *Int J Radiat Oncol Biol Phys* 2010;76:460–466.
[150] Nakamura M, Fukumitsu N, Kamizawa S. A validated proton beam therapy patch-field protocol for effective treatment of large hepatocellular carcinoma. *J Radiat Res* 2018;59:632–638.
[151] Colbert LE, Cloyd JM, Koay EJ. Proton beam radiation as salvage therapy for bilateral colorectal liver metastases not amenable to second-stage hepatectomy. *Surgery* 2017;161:1543–1548.
[152] Lee CH, Hung SP, Hong JH. How small is TOO small? New liver constraint is needed- Proton therapy of hepatocellular carcinoma patients with small normal liver. *PLoS ONE* 2018;13:e0203854.
[153] Hsieh CE, Venkatesulu BP, Lee CH. Predictors of radiation-induced liver disease in eastern and western patients with hepatocellular carcinoma undergoing proton beam therapy. *Int J Radiat Oncol Biol Phys* 2019;105:73–86.
[154] Bert C, Durante M. Motion in radiotherapy: particle therapy. *Phys Med Biol* 2011;56:R113–R144.
[155] Fukuda K, Okumura T, Abei M. Long-term outcomes of proton beam therapy in patients with previously untreated hepatocellular carcinoma. *Cancer Sci* Mar 2017;108:497–503.
[156] Pfeiler T, Ahmad Khalil D, Ayadi M. Motion effects in proton treatments of hepatocellular carcinoma-4D robustly optimised pencil beam scanning plans versus double scattering plans. *Phys Med Biol* 2018;63:235006.
[157] McGowan SE, Burnet NG, Lomax AJ. Treatment planning optimisation in proton therapy. *Br J Radiol* 2013;86:20120288.
[158] Gérard JP, Conroy T, Bonnetain F. Preoperative radiotherapy with or without concurrent fluorouracil and leucovorin in T3-4 rectal cancers: results of FFCD 9203. *J Clin Oncol* 2006;24:4620–4625.
[159] Gray B, Van Hazel G, Hope M. Randomised trial of SIR-Spheres plus chemotherapy vs. chemotherapy alone for treating patients with liver metastases from primary large bowel cancer. *Ann Oncol* 2001;12:1711–1720.

Please cite this article as: N.K. Sharma *et al.*, The American Brachytherapy Society consensus statement for permanent implant brachytherapy using Yttrium-90 microsphere radioembolization for liver tumors, Brachytherapy, https://doi.org/10.1016/j.brachy.2022.04.004

[160] Van Hazel G, Blackwell A, Anderson J. Randomised phase 2 trial of SIR-Spheres plus fluorouracil/leucovorin chemotherapy versus fluorouracil/leucovorin chemotherapy alone in advanced colorectal cancer. *J Surg Oncol* 2004;88:78–85.

[161] Hendlisz A, Van den Eynde M, Peeters M. Phase III trial comparing protracted intravenous fluorouracil infusion alone or with yttrium-90 resin microspheres radioembolization for liver-limited metastatic colorectal cancer refractory to standard chemotherapy. *J Clin Oncol* 2010;28:3687–3694.

[162] van Hazel GA, Pavlakis N, Goldstein D. Treatment of fluorouracil-refractory patients with liver metastases from colorectal cancer by using yttrium-90 resin microspheres plus concomitant systemic irinotecan chemotherapy. *J Clin Oncol* 2009;27:4089–4095.

[163] Zou J, Zhu W, Meng H. Efficacy and safety of selective internal radiotherapy versus sorafenib for intermediate-locally advanced hepatocellular carcinoma: a systematic review and meta-analysis. *Expert Rev Gastroenterol Hepatol* 2019;13:271–279.

[164] Kennedy A, Brown DB, Feilchenfeldt J. Safety of selective internal radiation therapy (SIRT) with yttrium-90 microspheres combined with systemic anticancer agents: expert consensus. *J Gastrointest Oncol* 2017;8:1079–1099.

[165] Formenti SC, Demaria S. Combining radiotherapy and cancer immunotherapy: a paradigm shift. *J Natl Cancer Inst* 2013;105:256–265.

Please cite this article as: N.K. Sharma *et al.*, The American Brachytherapy Society consensus statement for permanent implant brachytherapy using Yttrium-90 microsphere radioembolization for liver tumors, Brachytherapy, https://doi.org/10.1016/j.brachy.2022.04.004